Uniaxial testing of expanded metal sheet

Juliana T. Oliveira, Joaquim O. Barros, Paulo B. Lourenço, A. Marques Pinho

Report 02-DEC/E-11

The present research has been carried out under
contract GROW-1999-70420 "ISO-BRICK" from the European Commission

DRAFT VERSION

Date: September 2002
No. of Pages: 32

Keywords: Expanded Metal Sheet, Mechanical characterization, anisotropy.

Escola de
Engenharia

Departamento de
Engenharia Civil

Universidade
do Minho

Azurém, 4800-085 Guimarães - Tel. +351 253 510 200 - Fax +351 253 510 217 - E-mail secG@civil.uminho.pt

Uniaxial testing of expanded metal sheet

Juliana T. Oliveira, Joaquim O. Barros, Paulo B. Lourenço, A. Marques Pinho

Report 02-DEC/E-11

The present research has been carried out under
contract GROW-1999-70420 "ISO-BRICK" from the European Commission

DRAFT VERSION

Date: September 2002
No. of Pages: 32

Keywords: Expanded Metal Sheet, Mechanical characterization, anisotropy.

Escola de
Engenharia

Departamento de
Engenharia Civil

Universidade
do Minho

Azurém, 4800-085 Guimarães - Tel. +351 253 510 200 - Fax +351 253 510 217 - E-mail secG@civil.uminho.pt

Contents

Azurém, P – 4800-058 Guimarães
Tel. +351 253 510200 • Fax +351 253 510217

Contents

Azurém, P – 4800-058 Guimarães Tel. +351 253 510200 • Fax +351 253 510217

1 Introduction

The present report is dedicated to characterize the tensile behavior of specimens of expanded metal sheet (EMS). To accomplish this purpose, direct tensile tests were carried out, in a first phase with EMS specimens, and in a second phase with mortar specimens reinforced with EMS. It was intended to use this EMS for reinforcing the concrete compression layer of brick masonry shells to be developed and characterized on the research project "ISO-BRICK". The EMS was provided by SUCERAM (Suministros Cerámicos del Vallés S.A.), a Spanish company, and partner of the aforementioned research project. The geometrical configuration of a rhomb module of the EMS is represented in Figure 1.1, where A and B are the larger and the smaller diagonals, and C and D are the width and the thickness of the metal strips. This EMS is identified by the reference 80/40/30/30 (A/B/C/D), where the two first dimensions are given in millimeters and the two last dimensions in tenths of millimeter.

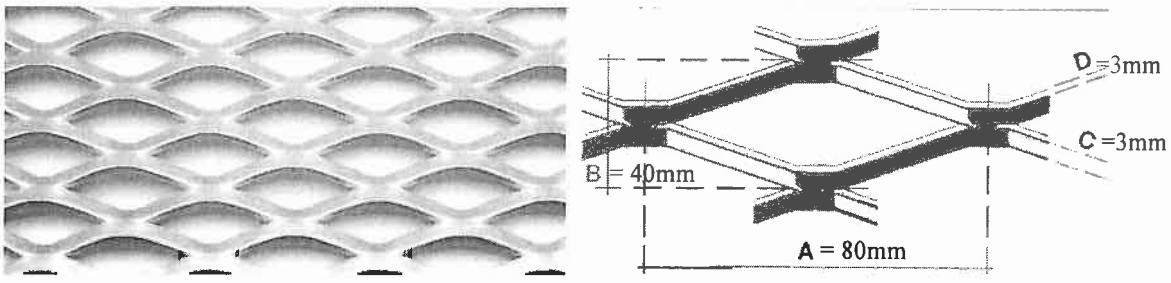

Figure 1.1 – Expanded Metal Sheet and geometry of its representative module.

Due to the geometrical anisotropy of the EMS, it was tested at different orientations with respect to the geometrical material axes G1 and G2 (different angle α between loading direction, L, and G1 geometrical axis), see Figure 1.2. G1 and G2 are oriented along the larger and the smaller diagonals of the rhomb, respectively. In Figure 1.2 it is

Azurém, P – 4800-058 Guimarães Tel. +351 253 510200 • Fax +351 253 510217

1 Introduction

The present report is dedicated to characterize the tensile behavior of specimens of expanded metal sheet (EMS). To accomplish this purpose, direct tensile tests were carried out, in a first phase with EMS specimens, and in a second phase with mortar specimens reinforced with EMS. It was intended to use this EMS for reinforcing the concrete compression layer of brick masonry shells to be developed and characterized on the research project "ISO-BRICK". The EMS was provided by SUCERAM (Suministros Cerámicos del Vallés S.A.), a Spanish company, and partner of the aforementioned research project. The geometrical configuration of a rhomb module of the EMS is represented in Figure 1.1, where A and B are the larger and the smaller diagonals, and C and D are the width and the thickness of the metal strips. This EMS is identified by the reference 80/40/30/30 (A/B/C/D), where the two first dimensions are given in millimeters and the two last dimensions in tenths of millimeter.

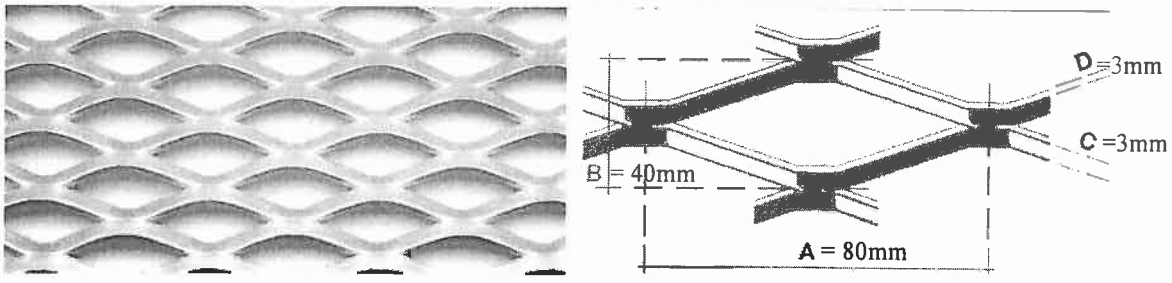

Figure 1.1 – Expanded Metal Sheet and geometry of its representative module.

Due to the geometrical anisotropy of the EMS, it was tested at different orientations with respect to the geometrical material axes G1 and G2 (different angle α between loading direction, L, and G1 geometrical axis), see Figure 1.2. G1 and G2 are oriented along the larger and the smaller diagonals of the rhomb, respectively. In Figure 1.2 it is

Azurém, P – 4800-058 Guimarães Tel. +351 253 510200 • Fax +351 253 510217

also represented the EMS material axes, M1 and M2. The EMS specimens were tested for angles α of 0, 30, 60 and 90°, setting four series. The specimens of mortar reinforced with EMS were tested for angles α of 0, 30 and 60°, setting three series. Each series is composed by three specimens.

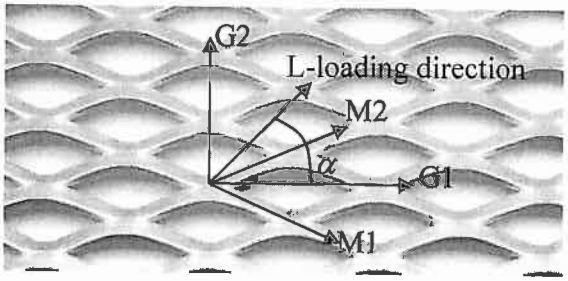

Figure 1.2 – Loading direction versus G1, G2 geometrical axes.

Azurém, P – 4800-058 Guimarães
Tel. +351 253 510200 • Fax +351 253 510217

also represented the EMS material axes, M1 and M2. The EMS specimens were tested for angles α of 0, 30, 60 and 90°, setting four series. The specimens of mortar reinforced with EMS were tested for angles α of 0, 30 and 60°, setting three series. Each series is composed by three specimens.

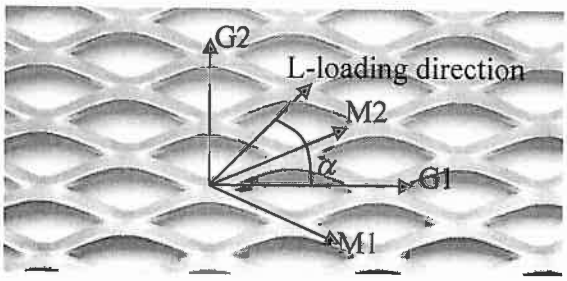

Figure 1.2 – Loading direction versus G1, G2 geometrical axes.

Azurém, P – 4800-058 Guimarães
Tel. +351 253 510200 • Fax +351 253 510217

2 Direct tensile tests on specimens of expanded metal sheet

2.1 Description of the test set-up

All specimens were cut with equal dimensions, at different orientation angles with respect to the material axes. The specimens had a width of 200mm, a full length of 500mm and a free testing length of 300mm, see Figure 2.1. At the extremities of the EMS specimens a strip of 100mm width was involved by appropriate "vulcanized" rubber of 15mm thick, in order to distribute the load applied by the machine load platens and to avoid excessive stress concentration.

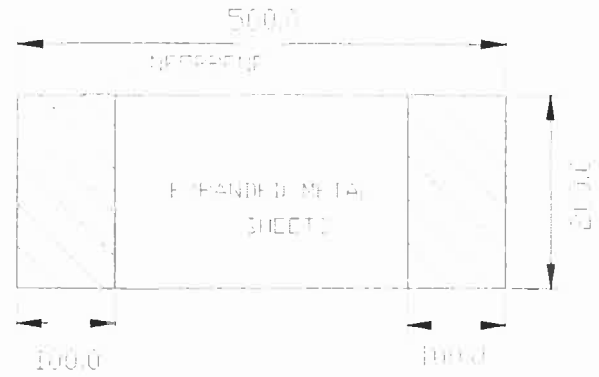

(a) (mm)

(b)

Figure 2.1 – Geometry of the EMS specimens: (a) dimensions (mm) and (b) photo. The specimens are shown horizontally but they have been tested vertically.

The specimens were tested in direct tension using a DARTEC universal testing machine with a load cell of 600kN maximum load bearing capacity, see Figure 2.2. At the end of the first tests carried out it was realized that this load cell could be unadjusted for

Azurém, P – 4800-058 Guimarães Tel. +351 253 510200 • Fax +351 253 510217

2 Direct tensile tests on specimens of expanded metal sheet

2.1 Description of the test set-up

All specimens were cut with equal dimensions, at different orientation angles with respect to the material axes. The specimens had a width of 200mm, a full length of 500mm and a free testing length of 300mm, see Figure 2.1. At the extremities of the EMS specimens a strip of 100mm width was involved by appropriate "vulcanized" rubber of 15mm thick, in order to distribute the load applied by the machine load platens and to avoid excessive stress concentration.

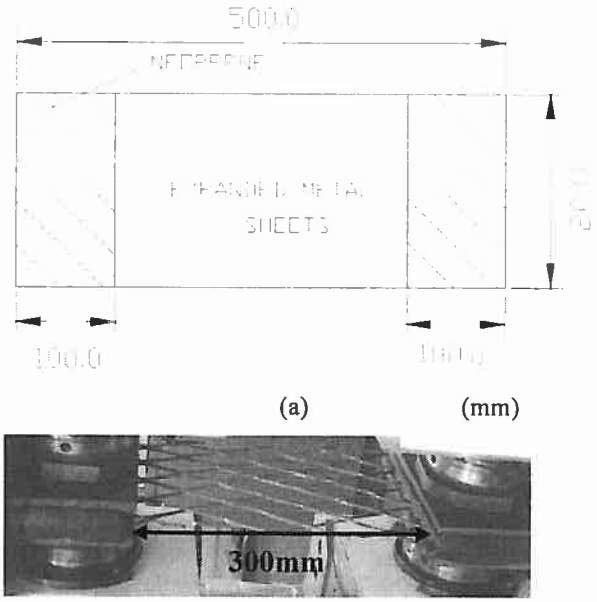

(a) (mm)

(b)

Figure 2.1 – Geometry of the EMS specimens: (a) dimensions (mm) and (b) photo. The specimens are shown horizontally but they have been tested vertically.

The specimens were tested in direct tension using a DARTEC universal testing machine with a load cell of 600kN maximum load bearing capacity, see Figure 2.2. At the end of the first tests carried out it was realized that this load cell could be unadjusted for

Azurém, P – 4800-058 Guimarães Tel. +351 253 510200 • Fax +351 253 510217

the specimens tested, because the maximum load attained was about 35kN, well below the load bearing capacity of this load cell. Therefore, some errors could be registered in the force values measured by this load cell. To assess the amount of this error, a correlation was made between the force values measured on an external load cell of 25 kN load bearing capacity and on the machine internal load cell, see Figure 2.3 and Figure 2.4. From the results obtained it was verified that DARTEC load cell registered values 1.24%, 0.80% and 0.60% lower than the values measured by the external load cell, for loading regimes of 0-6kN, 6-14kN and 14-20kN, respectively. Therefore it was assumed that the internal load cell of DARTEC has enough accuracy on the loading regime applied on the tests carried out with EMS specimens.

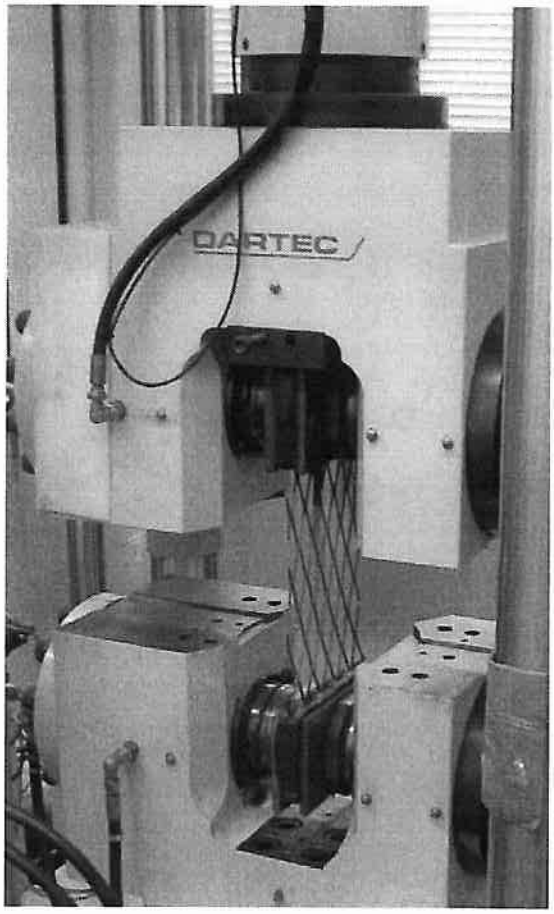

Figure 2.2 –EMS specimen mounted on the testing machine.

Azurém, P – 4800-058 Guimarães
Tel. +351 253 510200 • Fax +351 253 510217

the specimens tested, because the maximum load attained was about 35kN, well below the load bearing capacity of this load cell. Therefore, some errors could be registered in the force values measured by this load cell. To assess the amount of this error, a correlation was made between the force values measured on an external load cell of 25 kN load bearing capacity and on the machine internal load cell, see Figure 2.3 and Figure 2.4. From the results obtained it was verified that DARTEC load cell registered values 1.24%, 0.80% and 0.60% lower than the values measured by the external load cell, for loading regimes of 0-6kN, 6-14kN and 14-20kN, respectively. Therefore it was assumed that the internal load cell of DARTEC has enough accuracy on the loading regime applied on the tests carried out with EMS specimens.

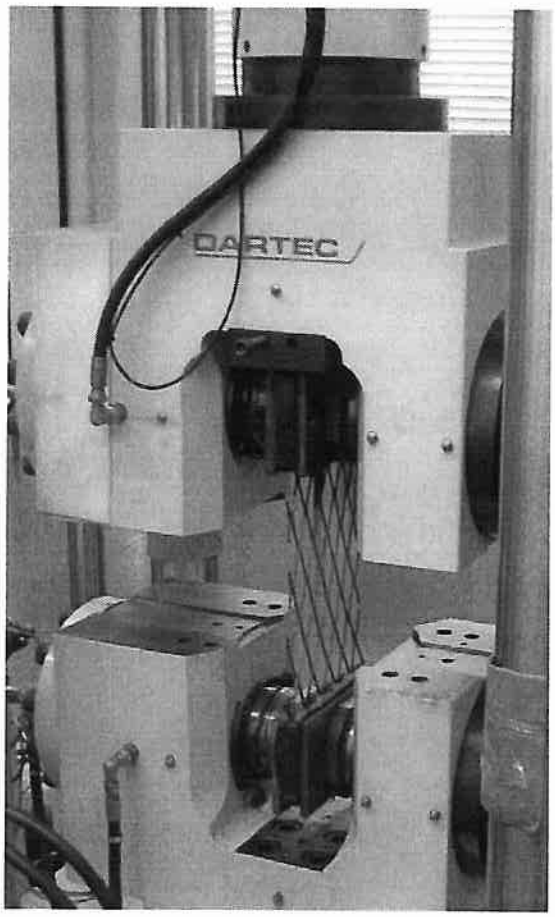

Figure 2.2 –EMS specimen mounted on the testing machine.

Azurém, P – 4800-058 Guimarães
Tel. +351 253 510200 • Fax +351 253 510217

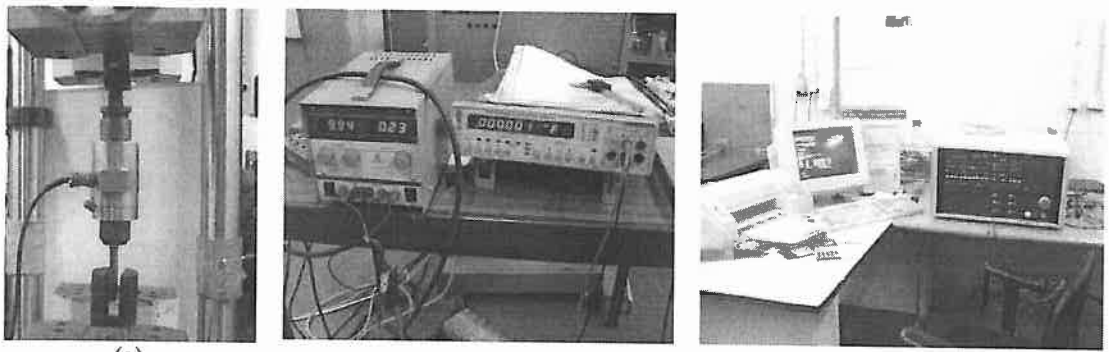

(a) (b) (c)

Figure 2.3 – Test set up to assess the confidence of the values registered on the DARTEC internal load cell on the tests with the EMS: (a) load cell of 25 kN load bearing capacity; (b) SENSOTEC system; (b) DARTEC system.

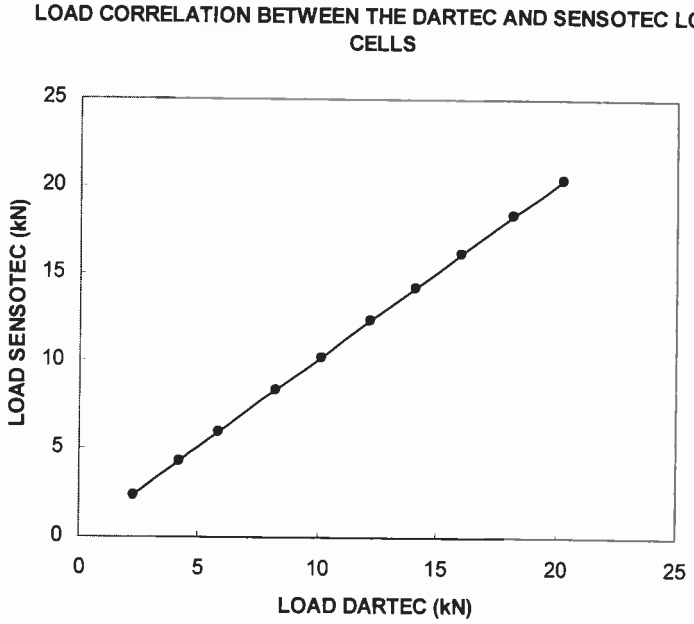

Figure 2.4 – Relationship between the forces registered on the DARTEC and SENSOTEC load cells.

The direct tensile tests on EMS were carried out on steps under load control. At the end of each loading step, the load was maintained constant during a period of time necessary for measuring the mesh geometry variation, using an electronic meter. The specimens were fixed to the equipment using steel claws designed for this purpose, in order that the contact area of the claws coincides with the strips of vulcanized rubber.

The longitudinal deformation of the EMS specimens was measured using the internal DARTEC displacement transducer. The values registered by this transducer

Azurém, P – 4800-058 Guimarães
Tel. +351 253 510200 • Fax +351 253 510217

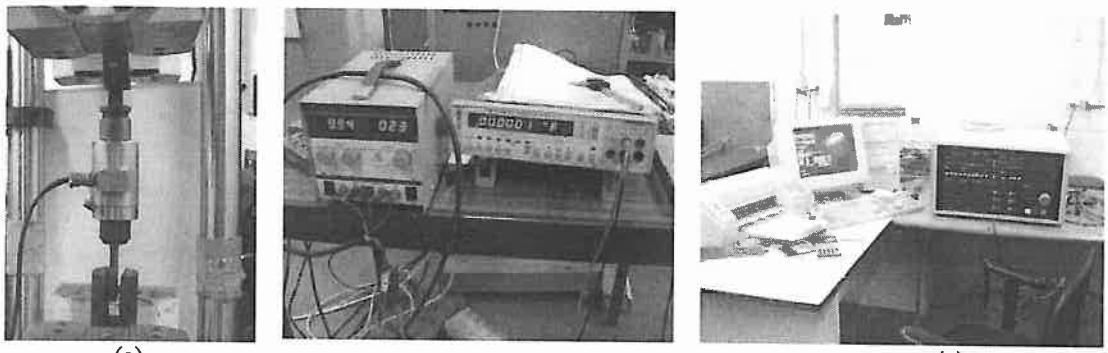

(a) (b) (c)

Figure 2.3 – Test set up to assess the confidence of the values registered on the DARTEC internal load cell on the tests with the EMS: (a) load cell of 25 kN load bearing capacity; (b) SENSOTEC system; (b) DARTEC system.

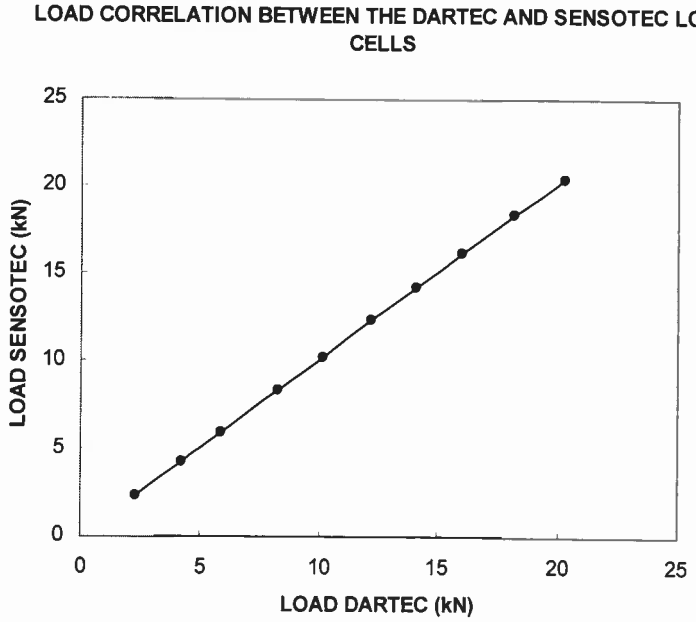

Figure 2.4 – Relationship between the forces registered on the DARTEC and SENSOTEC load cells.

The direct tensile tests on EMS were carried out on steps under load control. At the end of each loading step, the load was maintained constant during a period of time necessary for measuring the mesh geometry variation, using an electronic meter. The specimens were fixed to the equipment using steel claws designed for this purpose, in order that the contact area of the claws coincides with the strips of vulcanized rubber.

The longitudinal deformation of the EMS specimens was measured using the internal DARTEC displacement transducer. The values registered by this transducer

Azurém, P – 4800-058 Guimarães
Tel. +351 253 510200 • Fax +351 253 510217

includes, not only the deformation of the material, but also the geometry accommodation of the mesh.

2.2 Results

For each one of the testing directions (0°, 30°, 60° and 90°), three EMS specimens were tested.

2.2.1 EMS tested at an angle of 0°

In these EMS specimens the loading direction coincides with the G1 EMS geometrical axis, see Figure 2.5. These specimens have shown significant changes in their geometry and reached an average maximum load of approximately 12kN. Figure 2.5 illustrates the changes in the geometry during the loading process, indicating that collapse occurred in the transition area of the rhomb, near the nodes of the EMS.

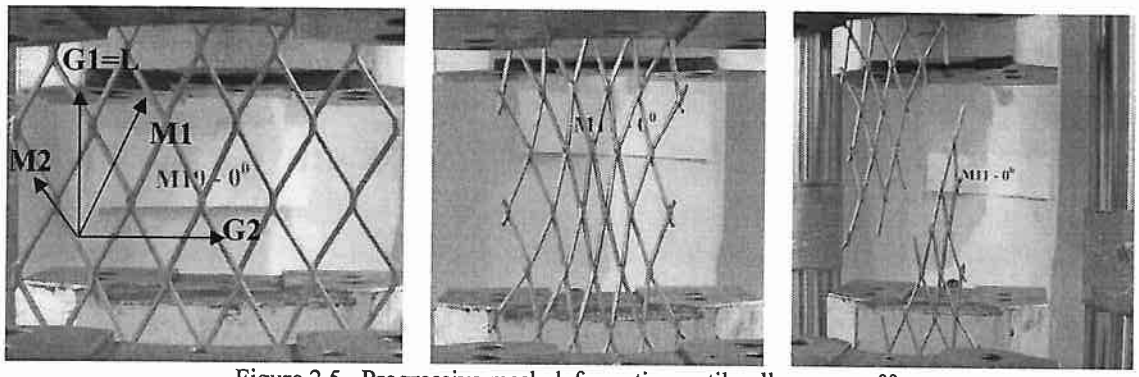

Figure 2.5– Progressive mesh deformation until collapse, $\alpha = 0°$.

Figure 2.6 shows the results in terms of load-displacement relationship. The displacements at peak load and at ultimate load are rather large, and the maximum load attained considerable values. Table 2.1 includes the limit of proportionality at 0.2%, σ_L, (see Figure 2.7) and its strain, ε_L, the peak stress, σ_p, and its strain, ε_p, and the ultimate strain, ε_u. The stress was obtained dividing the load by the cross section area of the EMS wires composing the specimen cross-section. The strain was determined dividing the displacement by the free testing length (300mm). The test on specimen M10 was prematurely interrupted due to problems with the data acquisition system.

Azurém, P – 4800-058 Guimarães
Tel. +351 253 510200 • Fax +351 253 510217

includes, not only the deformation of the material, but also the geometry accommodation of the mesh.

2.2 Results

For each one of the testing directions (0°, 30°, 60° and 90°), three EMS specimens were tested.

2.2.1 EMS tested at an angle of 0°

In these EMS specimens the loading direction coincides with the G1 EMS geometrical axis, see Figure 2.5. These specimens have shown significant changes in their geometry and reached an average maximum load of approximately 12kN. Figure 2.5 illustrates the changes in the geometry during the loading process, indicating that collapse occurred in the transition area of the rhomb, near the nodes of the EMS.

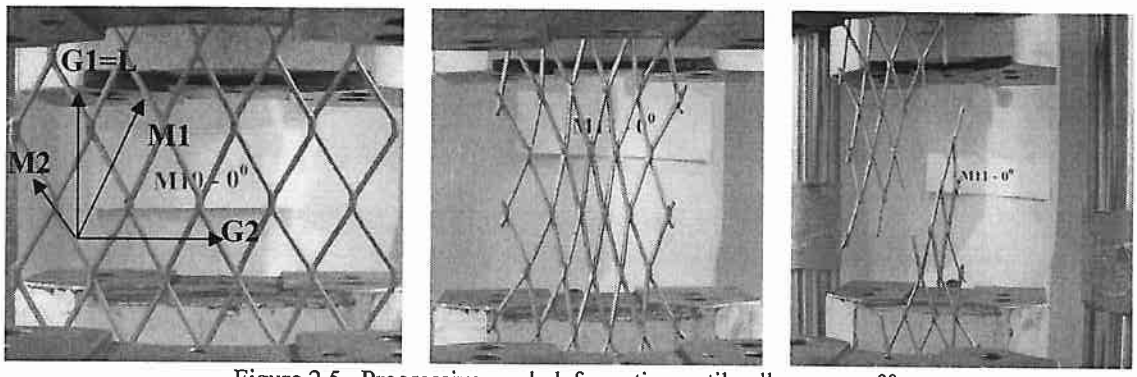

Figure 2.5– Progressive mesh deformation until collapse, $\alpha = 0°$.

Figure 2.6 shows the results in terms of load-displacement relationship. The displacements at peak load and at ultimate load are rather large, and the maximum load attained considerable values. Table 2.1 includes the limit of proportionality at 0.2%, σ_L, (see Figure 2.7) and its strain, ε_L, the peak stress, σ_p, and its strain, ε_p, and the ultimate strain, ε_u. The stress was obtained dividing the load by the cross section area of the EMS wires composing the specimen cross-section. The strain was determined dividing the displacement by the free testing length (300mm). The test on specimen M10 was prematurely interrupted due to problems with the data acquisition system.

Azurém, P – 4800-058 Guimarães
Tel. +351 253 510200 • Fax +351 253 510217

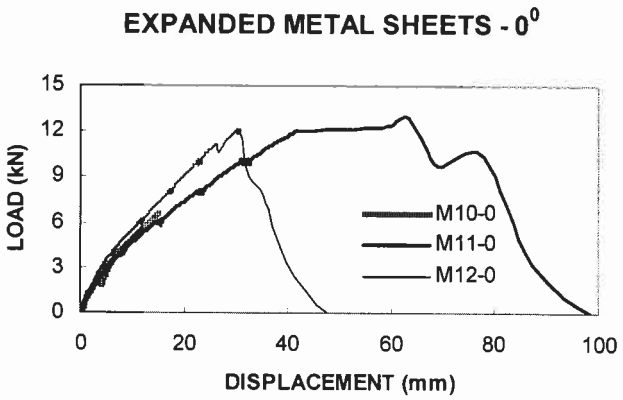

Figure 2.6 – Load-displacement diagrams for $\alpha = 0°$.

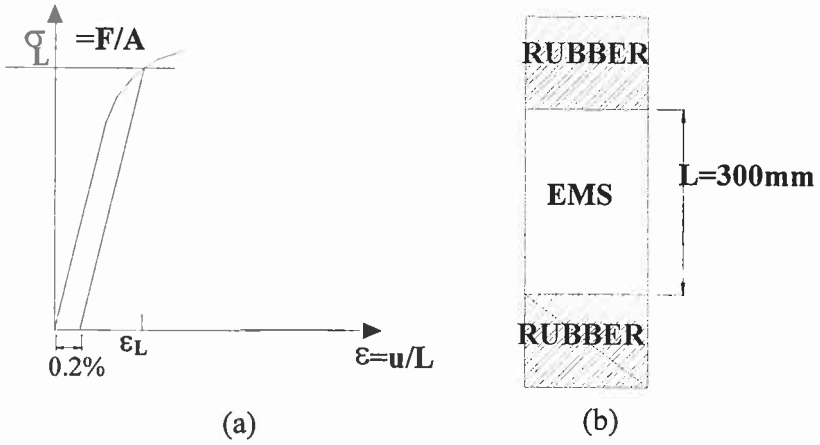

Figure 2.7 – Limit of proportionality at 0.2%: (a) how was evaluated; (b) free testing length of the EMS specimen.

Table 2.1 – Main results from the tests with EMS specimens loaded at 0°.

Specimen	Limit of proportionality, σ_L [MPa]	Strain at limit of proportionality, ε_L [%]	Peak stress, σ_p [MPa]	Strain at peak stress ε_p [%]	Ultimate strain ε_u [%]
M10	37.24	1.80	-	-	-
M11	45.52	2.80	133.79	13.90	21.00
M12	43.04	2.00	131.74	10.00	10.00
Average	41.93	2.20	132.77	12.00	15.50

Analyzing the results on Table 2.1 it was verified that the strains are rather large because the displacements used on its evaluation includes the geometry accommodation of the

Azurém, P – 4800-058 Guimarães
Tel. +351 253 510200 • Fax +351 253 510217

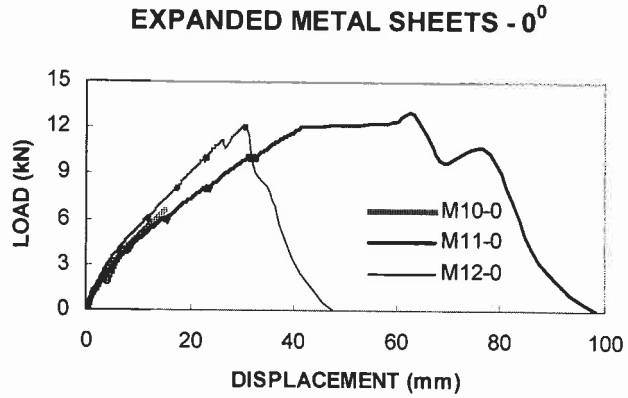

Figure 2.6 – Load-displacement diagrams for $\alpha = 0°$.

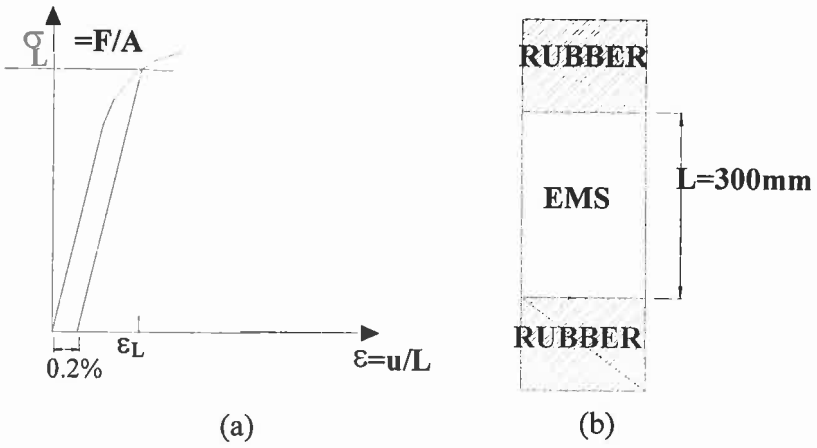

Figure 2.7 – Limit of proportionality at 0.2%: (a) how was evaluated; (b) free testing length of the EMS specimen.

Table 2.1 – Main results from the tests with EMS specimens loaded at 0°.

Specimen	Limit of proportionality, σ_L [MPa]	Strain at limit of proportionality, ε_L [%]	Peak stress, σ_p [MPa]	Strain at peak stress ε_p [%]	Ultimate strain ε_u [%]
M10	37.24	1.80	-	-	-
M11	45.52	2.80	133.79	13.90	21.00
M12	43.04	2.00	131.74	10.00	10.00
Average	41.93	2.20	132.77	12.00	15.50

Analyzing the results on Table 2.1 it was verified that the strains are rather large because the displacements used on its evaluation includes the geometry accommodation of the

Azurém, P – 4800-058 Guimarães
Tel. +351 253 510200 • Fax +351 253 510217

EMS specimen. Therefore it is a fictitious strain, not representative of the strains occurred on the wires of the EMS specimen. Even the strain at 0.2%, ε_L, is much higher than the values obtained on steel rebars, showing a significant variation of the geometry of the EMS specimen for this level of deformation. The stresses at the limit of proportionality is about 30% of the peak stress revealing that, for acceptable deformations the EMS sustains a reduced stress level.

2.2.2 EMS tested at an angle of 30°

In these EMS specimens the loading direction makes 30° with the G1 EMS geometrical axis, see Figure 2.8. Since the loading direction coincides with the M2 EMS material direction, the deformation of the EMS specimens was much lower than the deformation registered in previous EMS specimens. The deformation of the present specimens has a major contribution from the strains of the wires at the material M2 axis. These wires have resisted to the load applied. The contribution of the wires on the material M1 direction for the load bearing capacity of the EMS specimen was marginal. The maximum load has also attained an average value of about 12kN.

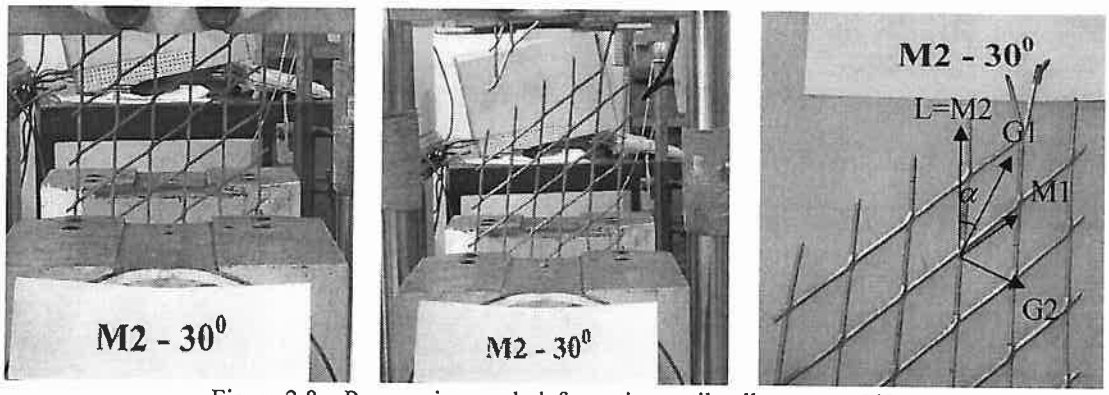

Figure 2.8 – Progressive mesh deformation until collapse, $\alpha = 30°$.

The load-displacement relationships registered on the EMS specimens, loaded at α=30°, are shown in Figure 2.9. Problems with the data acquisition system prevented to record the results of the M3-30 specimen, but its behavior was similar to the others two

Azurém, P – 4800-058 Guimarães
Tel. +351 253 510200 • Fax +351 253 510217

EMS specimen. Therefore it is a fictitious strain, not representative of the strains occurred on the wires of the EMS specimen. Even the strain at 0.2%, ε_L, is much higher than the values obtained on steel rebars, showing a significant variation of the geometry of the EMS specimen for this level of deformation. The stresses at the limit of proportionality is about 30% of the peak stress revealing that, for acceptable deformations the EMS sustains a reduced stress level.

2.2.2 EMS tested at an angle of 30°

In these EMS specimens the loading direction makes 30° with the G1 EMS geometrical axis, see Figure 2.8. Since the loading direction coincides with the M2 EMS material direction, the deformation of the EMS specimens was much lower than the deformation registered in previous EMS specimens. The deformation of the present specimens has a major contribution from the strains of the wires at the material M2 axis. These wires have resisted to the load applied. The contribution of the wires on the material M1 direction for the load bearing capacity of the EMS specimen was marginal. The maximum load has also attained an average value of about 12kN.

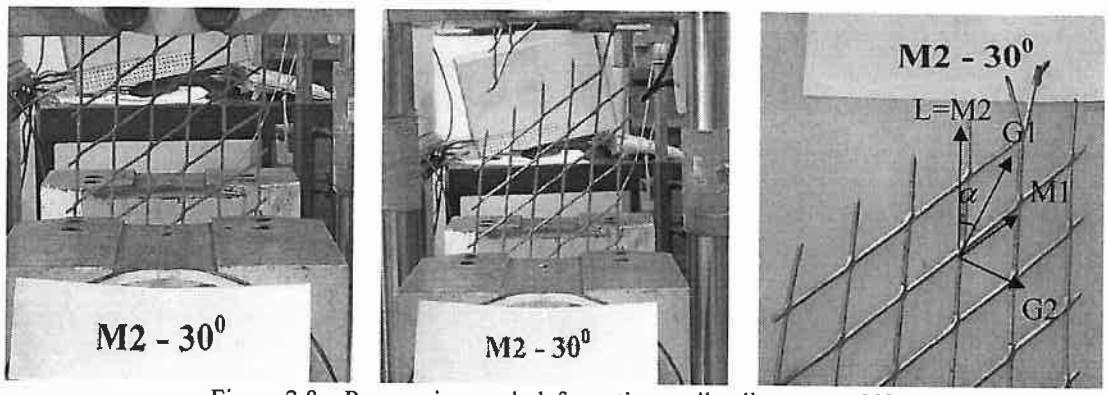

Figure 2.8 – Progressive mesh deformation until collapse, $\alpha = 30°$.

The load-displacement relationships registered on the EMS specimens, loaded at α=30°, are shown in Figure 2.9. Problems with the data acquisition system prevented to record the results of the M3-30 specimen, but its behavior was similar to the others two

Azurém, P – 4800-058 Guimarães
Tel. +351 253 510200 • Fax +351 253 510217

specimens. In spite of the displacement at peak load of this series is significantly smaller than the values registered on the series of specimens at 0°, the maximum load was similar on both series. The relationship between the load and the displacement registered on the specimens of this series is much more linear, than the one of the specimens of previous series, because the geometry variation of the EMS specimens loaded at α=30° was much lower.

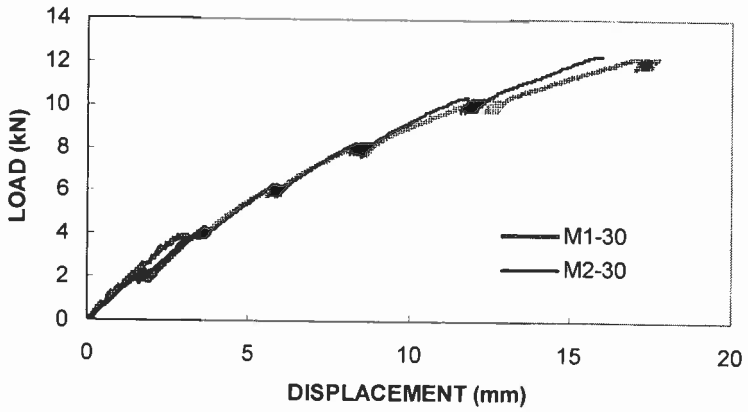

Figure 2.9 – Load-displacement diagrams for $\alpha = 30°$.

Table 2.2 includes the main data obtained on the tests with the specimens of this series. The stresses at the limit of proportionality and at peak load are higher than the corresponding values of the previous series. However, the limit of proportionality is still about 30% of the peak stress.

Table 2.2 – Main results from the tests with EMS specimens loaded at 30°.

Specimen	Limit of proportionality, σ_L [MPa]	Strain at limit of proportionality, ε_L [%]	Peak stress, σ_p [MPa]	Strain at peak stress ε_p [%]	Ultimate strain ε_u [%]
M1	67.39	1.00	202.17	5.50	5.90
M2	67.39	1.10	206.52	5.30	5.30
Average	67.39	1.05	204.35	5.40	5.60

2.2.3 EMS tested at an angle of 60°

In these EMS specimens the loading direction makes 60° with the G1 EMS geometrical axis, see Figure 2.10. In comparison to previous series of specimens, in this

Azurém, P – 4800-058 Guimarães
Tel. +351 253 510200 • Fax +351 253 510217

specimens. In spite of the displacement at peak load of this series is significantly smaller than the values registered on the series of specimens at 0°, the maximum load was similar on both series. The relationship between the load and the displacement registered on the specimens of this series is much more linear, than the one of the specimens of previous series, because the geometry variation of the EMS specimens loaded at α=30° was much lower.

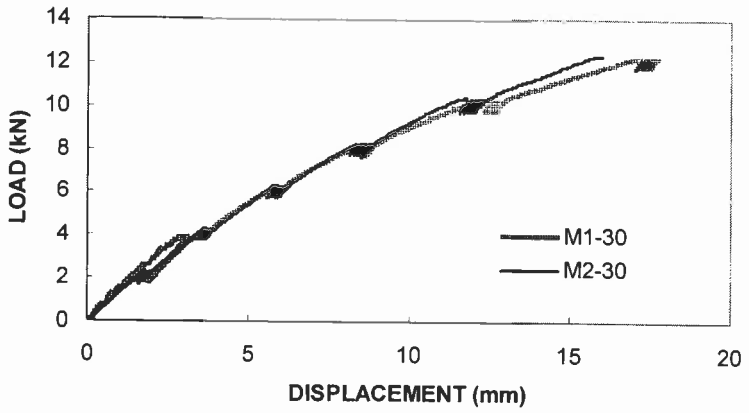

Figure 2.9 – Load-displacement diagrams for $\alpha = 30°$.

Table 2.2 includes the main data obtained on the tests with the specimens of this series. The stresses at the limit of proportionality and at peak load are higher than the corresponding values of the previous series. However, the limit of proportionality is still about 30% of the peak stress.

Table 2.2 – Main results from the tests with EMS specimens loaded at 30°.

Specimen	Limit of proportionality, σ_L [MPa]	Strain at limit of proportionality, ε_L [%]	Peak stress, σ_p [MPa]	Strain at peak stress ε_p [%]	Ultimate strain ε_u [%]
M1	67.39	1.00	202.17	5.50	5.90
M2	67.39	1.10	206.52	5.30	5.30
Average	67.39	1.05	204.35	5.40	5.60

2.2.3 EMS tested at an angle of 60°

In these EMS specimens the loading direction makes 60° with the G1 EMS geometrical axis, see Figure 2.10. In comparison to previous series of specimens, in this

Azurém, P – 4800-058 Guimarães
Tel. +351 253 510200 • Fax +351 253 510217

one the material axis M1 and M2 have the highest inclination to the loading direction. Consequently, the present specimens had higher deformation, having attained at the end of the test a length two times the initial length of the specimen. The major contribution for the mesh deformation resulted from the geometry accommodation to the load applied. The average value of the maximum load was about 3.9kN. At rupture, some wires embedded into the vulcanized rubber have failed by slipping (see Figure 2.10).

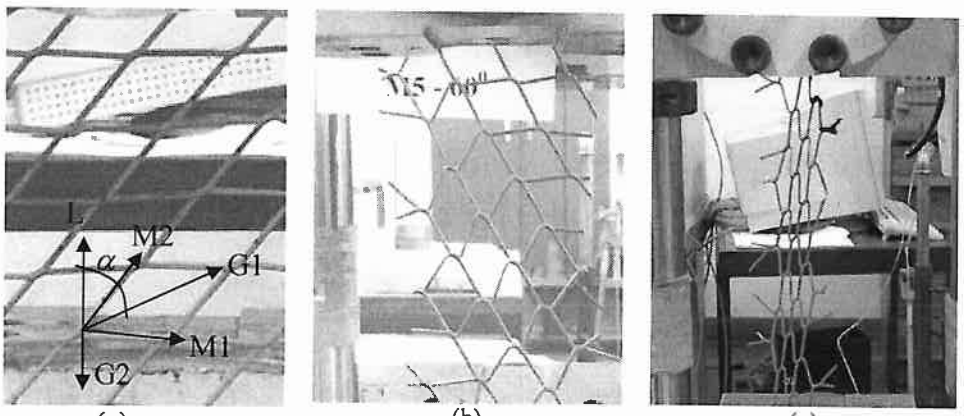

(a) (b) (c)

Figure 2.10 – Progressive mesh deformation until collapse, $\alpha = 60°$.

Figure 2.11 represents the load-displacement relationship obtained on the EMS specimens at 60°. The deformation was the highest and the ultimate load was the lowest values amongst the series analyzed up to the present point. After a linear branch, the load increased smoothly up to a deflection of about 150mm, showing a reduced stiffness due to EMS geometry accommodation. After this deformation the stiffness of the responses has increased because the EMS specimens became too stretched (see Figure 2.10c). Unload-reload branches have occurred, coinciding with the EMS geometry accommodation.

Azurém, P – 4800-058 Guimarães
Tel. +351 253 510200 • Fax +351 253 510217

one the material axis M1 and M2 have the highest inclination to the loading direction. Consequently, the present specimens had higher deformation, having attained at the end of the test a length two times the initial length of the specimen. The major contribution for the mesh deformation resulted from the geometry accommodation to the load applied. The average value of the maximum load was about 3.9kN. At rupture, some wires embedded into the vulcanized rubber have failed by slipping (see Figure 2.10).

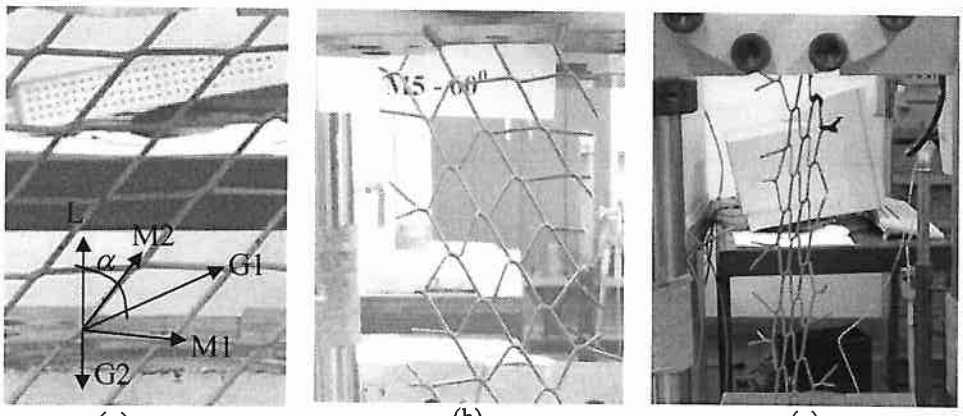

(a) (b) (c)

Figure 2.10 – Progressive mesh deformation until collapse, $\alpha = 60°$.

Figure 2.11 represents the load-displacement relationship obtained on the EMS specimens at 60°. The deformation was the highest and the ultimate load was the lowest values amongst the series analyzed up to the present point. After a linear branch, the load increased smoothly up to a deflection of about 150mm, showing a reduced stiffness due to EMS geometry accommodation. After this deformation the stiffness of the responses has increased because the EMS specimens became too stretched (see Figure 2.10c). Unload-reload branches have occurred, coinciding with the EMS geometry accommodation.

Azurém, P – 4800-058 Guimarães
Tel. +351 253 510200 • Fax +351 253 510217

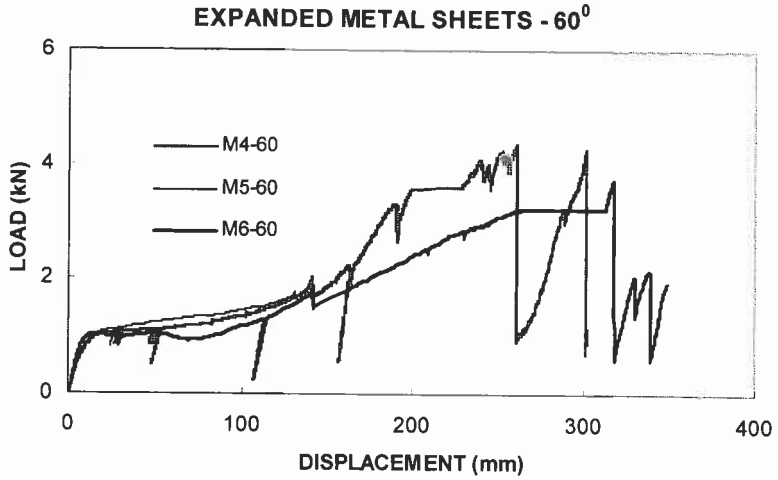

Figure 2.11 – Load-displacement diagrams for $\alpha = 60°$.

Table 2.3 includes the main data obtained on the tests with the specimens of this series. The stress values at the limit of proportionality and at peak stress are too low, with σ_L being about 60% of the σ_p.

Table 2.3 – Main results from the tests with EMS specimens loaded at 60°.

Specimen	Limit of proportionality, σ_L [MPa]	Strain at limit of proportionality, ε_L [%]	Peak stress, σ_p [MPa]	Strain at peak stress ε_p [%]	Ultimate strain ε_u [%]
M4	13.68	1.90	26.16	14.8	47.10
M5	16.52	2.60	26.16	8.70	43.60
M6	20.26	1.50	-	-	10.50
Average	16.82	2.00	26.16	11.8	33.73

2.2.4 Mesh tested at 90° angle

The behavior of the EMS specimens tested at 90° and 60° was similar, but the geometry accommodation of the specimens loaded at 90° was even greater, see Figure 2.12.

Azurém, P – 4800-058 Guimarães
Tel. +351 253 510200 • Fax +351 253 510217

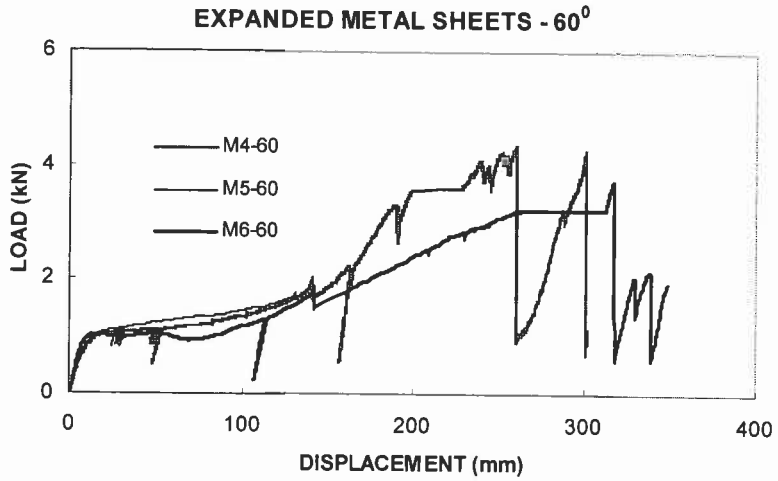

Figure 2.11 – Load-displacement diagrams for $\alpha = 60°$.

Table 2.3 includes the main data obtained on the tests with the specimens of this series. The stress values at the limit of proportionality and at peak stress are too low, with σ_L being about 60% of the σ_p.

Table 2.3 – Main results from the tests with EMS specimens loaded at 60°.

Specimen	Limit of proportionality, σ_L [MPa]	Strain at limit of proportionality, ε_L [%]	Peak stress, σ_p [MPa]	Strain at peak stress ε_p [%]	Ultimate strain ε_u [%]
M4	13.68	1.90	26.16	14.8	47.10
M5	16.52	2.60	26.16	8.70	43.60
M6	20.26	1.50	-	-	10.50
Average	16.82	2.00	26.16	11.8	33.73

2.2.4 Mesh tested at 90° angle

The behavior of the EMS specimens tested at 90° and 60° was similar, but the geometry accommodation of the specimens loaded at 90° was even greater, see Figure 2.12.

Azurém, P – 4800-058 Guimarães
Tel. +351 253 510200 • Fax +351 253 510217

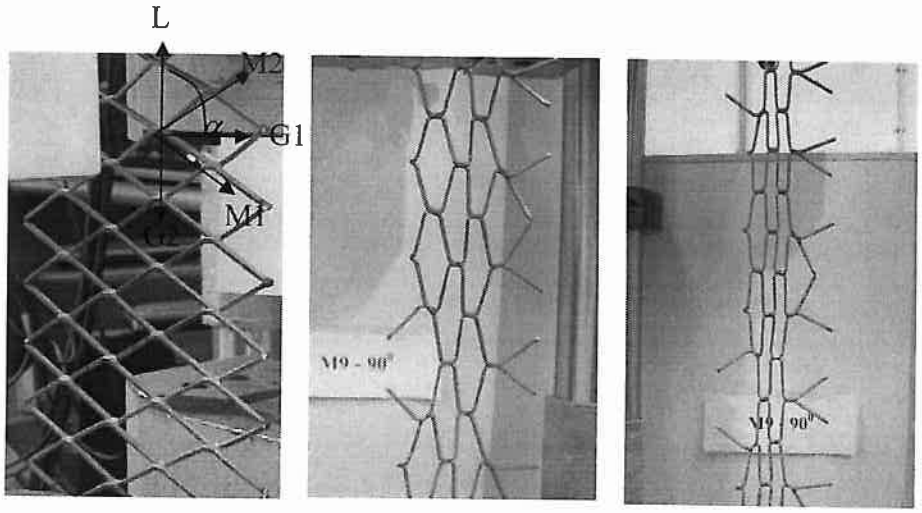

Figure 2.12 – Progressive mesh deformation until collapse, $\alpha = 90°$.

The load-displacement relationship registered on EMS specimens loaded at 90° was represented on Figure 2.13 It was verified that, at a load of about 0.5kN a significant increment on the deformation has occurred without appreciable load increment. This phase corresponds to the geometry accommodation of the specimen. After this phase, the specimens M7 and M8 have shown a significant increment on the stiffness of their responses, corresponding to the phase where the wires of the EMS specimen were aligned to the loading direction (see Figure 2.12). Specimen M7 has failed for a load of 4,0kN when the displacement was 351,9mm, while specimen M8 failed at a load of 4,5kN, for a displacement of 368,8mm. The test on specimen M9 was interrupted when the load and the corresponding displacement was 4,8kN and 286,8mm, respectively.

Azurém, P – 4800-058 Guimarães
Tel. +351 253 510200 • Fax +351 253 510217

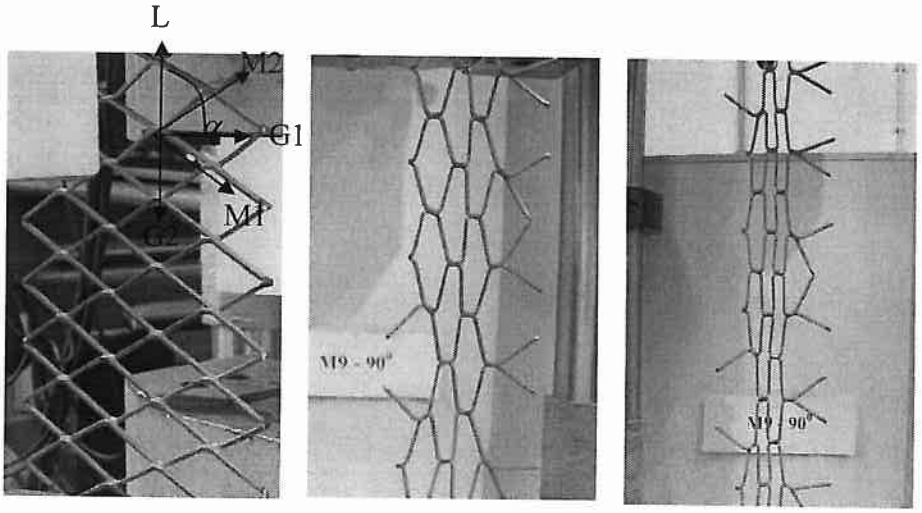

Figure 2.12 – Progressive mesh deformation until collapse, $\alpha = 90°$.

The load-displacement relationship registered on EMS specimens loaded at 90° was represented on Figure 2.13 It was verified that, at a load of about 0.5kN a significant increment on the deformation has occurred without appreciable load increment. This phase corresponds to the geometry accommodation of the specimen. After this phase, the specimens M7 and M8 have shown a significant increment on the stiffness of their responses, corresponding to the phase where the wires of the EMS specimen were aligned to the loading direction (see Figure 2.12). Specimen M7 has failed for a load of 4,0kN when the displacement was 351,9mm, while specimen M8 failed at a load of 4,5kN, for a displacement of 368,8mm. The test on specimen M9 was interrupted when the load and the corresponding displacement was 4,8kN and 286,8mm, respectively.

Azurém, P – 4800-058 Guimarães
Tel. +351 253 510200 • Fax +351 253 510217

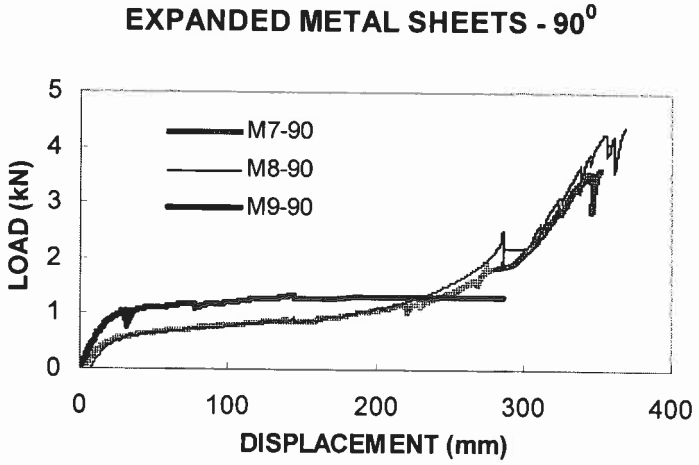

Figure 2.13 – Force-displacement diagrams for $\alpha = 90°$.

Table 2.4 includes the main data obtained on the tests with the specimens of this series. Similar to EMS specimens loaded at 60°, the stress values at the limit of proportionality and at peak stress are also too low, with σ_L being about 50% of the σ_p, and the deformability was too high.

Table 2.4 – Main results from the tests with EMS specimens loaded at 90°.

Specimen	Limit of proportionality, σ_L [MPa]	Strain at limit of proportionality, ε_L [%]	Peak stress, σ_p [MPa]	Strain at peak stress ε_p [%]	Ultimate strain ε_u [%]
M7	12.11	2.60	23.44	44.60	46.1
M8	12.63	2.30	23.44	44.60	46.1
M9	12.50	3.20	27.79	22.70	48.2
Average	12.41	2.70	24.89	37.30	46.8

2.2.5 Equivalent conventional reinforcement

Taking the values of the forces at limit of proportionality and at peak load obtained on the tests carried out, an equivalent cross-section area, Aseq, of a fictitious S400 conventional steel bars was evaluated for these two load levels. The results obtained are included in Table 2.5.

Azurém, P – 4800-058 Guimarães
Tel. +351 253 510200 • Fax +351 253 510217

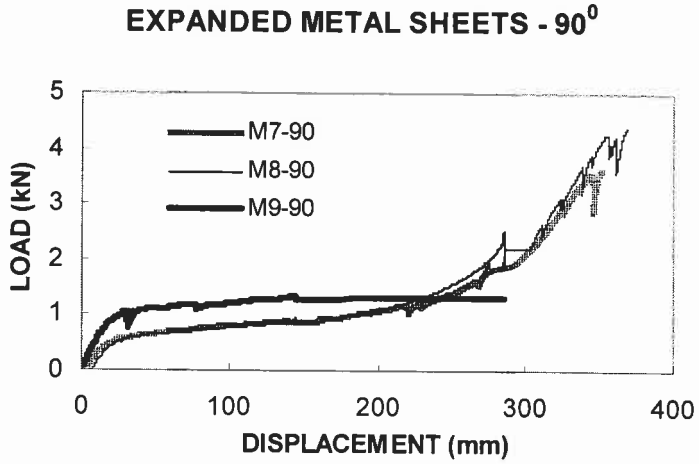

Figure 2.13 – Force-displacement diagrams for $\alpha = 90°$.

Table 2.4 includes the main data obtained on the tests with the specimens of this series. Similar to EMS specimens loaded at 60°, the stress values at the limit of proportionality and at peak stress are also too low, with σ_L being about 50% of the σ_p, and the deformability was too high.

Table 2.4 – Main results from the tests with EMS specimens loaded at 90°.

Specimen	Limit of proportionality, σ_L [MPa]	Strain at limit of proportionality, ε_L [%]	Peak stress, σ_p [MPa]	Strain at peak stress ε_p [%]	Ultimate strain ε_u [%]
M7	12.11	2.60	23.44	44.60	46.1
M8	12.63	2.30	23.44	44.60	46.1
M9	12.50	3.20	27.79	22.70	48.2
Average	12.41	2.70	24.89	37.30	46.8

2.2.5 Equivalent conventional reinforcement

Taking the values of the forces at limit of proportionality and at peak load obtained on the tests carried out, an equivalent cross-section area, Aseq, of a fictitious S400 conventional steel bars was evaluated for these two load levels. The results obtained are included in Table 2.5.

Azurém, P – 4800-058 Guimarães
Tel. +351 253 510200 • Fax +351 253 510217

Table 2.5 – Correlation with standard steel bars

Direction	F_L [kN]	$A_{s,eq,\ 0.2\%}$ [cm²/m]	F_p [kN]	$A_{s,eq,\ p}$ [cm²/m]
0°	3.77	2ϕ6/m [0.6]	11.95	6ϕ6/m [1.68]
30°	4.04	2ϕ6/m [0.6]	12.26	6ϕ6/m [1.68]
60°	0.71	0.4ϕ6/m [0.11]	1.05	0.5ϕ6/m [0.14]
90°	0.52	0.3ϕ6/m [0.08]	1.10	0.5ϕ6/m [0.14]

It was verified that, for load level corresponding to the limit of proportionality, the EMS specimen is equivalent to a two bars of six millimeters of diameter when α=0° and 30°, and gives a marginal reinforcement contribution when α=60° and 90°. For the peak load the equivalent cross section area is considerable when α=0° and 30°, but this force is only attained for very large deformations, not mobilized on practical applications.

2.3 Deformability

To assess the geometry variation and the strains at localized zones of the EMS, displacement measures were taken in intervals of load increments of 2kN. Figure 2.14 shows the measures carried out: L1 and L2 to obtain the geometry variation along the smaller and the larger diagonal of a EMS module, respectively; L3 to evaluate the strain on one of the edges of this EMS module; L4 to estimate the influence of the EMS nodes on the deformation. The measures were done using an electronic meter.

Azurém, P – 4800-058 Guimarães
Tel. +351 253 510200 • Fax +351 253 510217

Table 2.5 – Correlation with standard steel bars

Direction	F_L [kN]	$A_{s,eq,\ 0.2\%}$ [cm²/m]	F_p [kN]	$A_{s,eq,\ p}$ [cm²/m]
0°	3.77	2ϕ6/m [0.6]	11.95	6ϕ6/m [1.68]
30°	4.04	2ϕ6/m [0.6]	12.26	6ϕ6/m [1.68]
60°	0.71	0.4ϕ6/m [0.11]	1.05	0.5ϕ6/m [0.14]
90°	0.52	0.3ϕ6/m [0.08]	1.10	0.5ϕ6/m [0.14]

It was verified that, for load level corresponding to the limit of proportionality, the EMS specimen is equivalent to a two bars of six millimeters of diameter when α=0° and 30°, and gives a marginal reinforcement contribution when α=60° and 90°. For the peak load the equivalent cross section area is considerable when α=0° and 30°, but this force is only attained for very large deformations, not mobilized on practical applications.

2.3 Deformability

To assess the geometry variation and the strains at localized zones of the EMS, displacement measures were taken in intervals of load increments of 2kN. Figure 2.14 shows the measures carried out: L1 and L2 to obtain the geometry variation along the smaller and the larger diagonal of a EMS module, respectively; L3 to evaluate the strain on one of the edges of this EMS module; L4 to estimate the influence of the EMS nodes on the deformation. The measures were done using an electronic meter.

Azurém, P – 4800-058 Guimarães
Tel. +351 253 510200 • Fax +351 253 510217

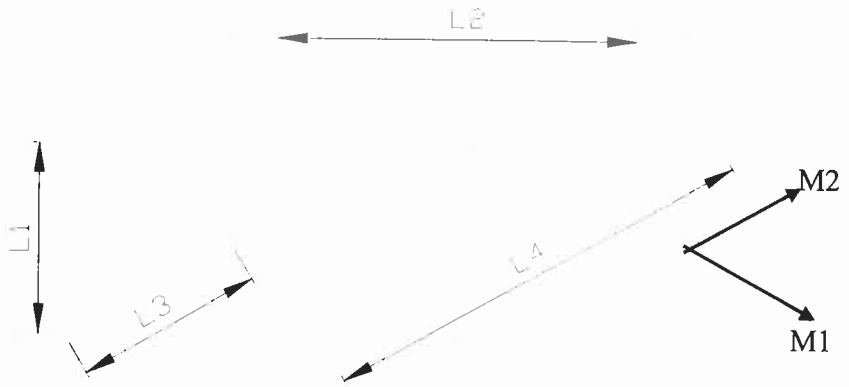

Figure 2.14 – Measurement points of displacement.

The variation of the smaller diagonal dimension of an EMS module, L1, was evaluated in all tests, and is represented in Figure 2.15. For 0° the length L1 decreased during the loading process because the direction of the smaller diagonal is orthogonal to the loading direction (see Figure 2.5). For 30° the variation of the L1 was marginal because the wires on the M2 material axis coincide with the loading direction. For 60° and 90° the direction of L1 approximates to the loading direction, resulting significant variations on the L1 length.

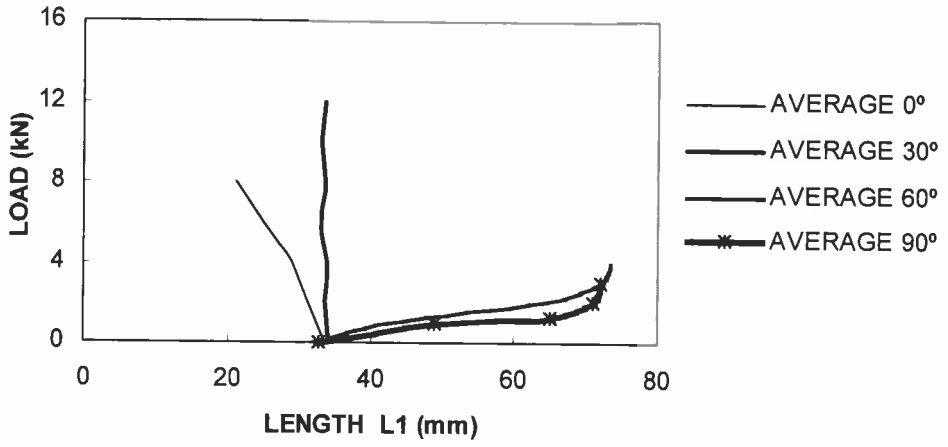

Figure 2.15 – Graphic load versus L1 length variation.

Azurém, P – 4800-058 Guimarães
Tel. +351 253 510200 • Fax +351 253 510217

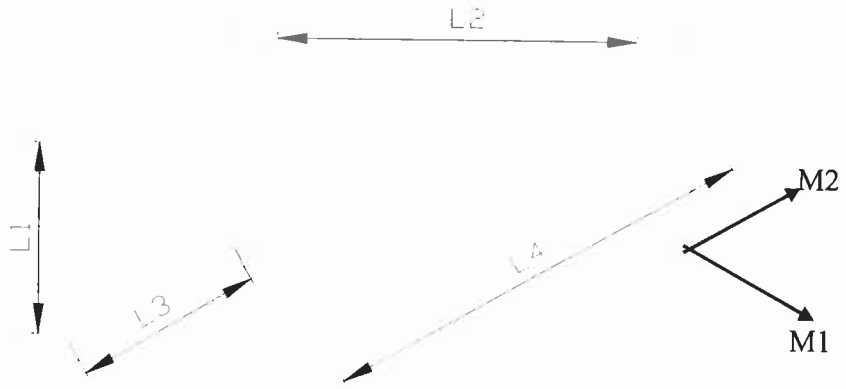

Figure 2.14 – Measurement points of displacement.

The variation of the smaller diagonal dimension of an EMS module, L1, was evaluated in all tests, and is represented in Figure 2.15. For 0° the length L1 decreased during the loading process because the direction of the smaller diagonal is orthogonal to the loading direction (see Figure 2.5). For 30° the variation of the L1 was marginal because the wires on the M2 material axis coincide with the loading direction. For 60° and 90° the direction of L1 approximates to the loading direction, resulting significant variations on the L1 length.

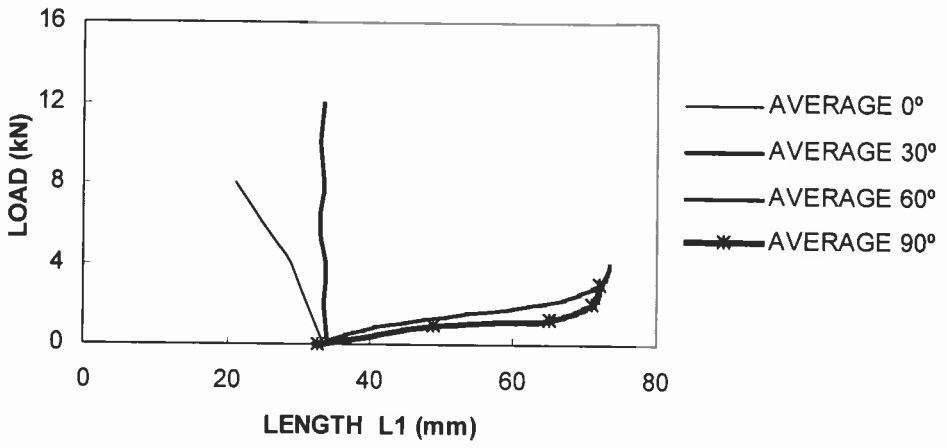

Figure 2.15 – Graphic load versus L1 length variation.

Azurém, P – 4800-058 Guimarães
Tel. +351 253 510200 • Fax +351 253 510217

Figure 2.16 represents the relationship between the load and the length variation on L2, i.e., in the larger diagonal of the EMS module. For specimens at 60° and 90° the L2 length variation has decreased in a similar shape (see also Figures 2.10 and 2.12). Difficulties achieved on measuring the specimens at 0° and 30° prevented the evaluation of the aforementioned relationship for these specimens.

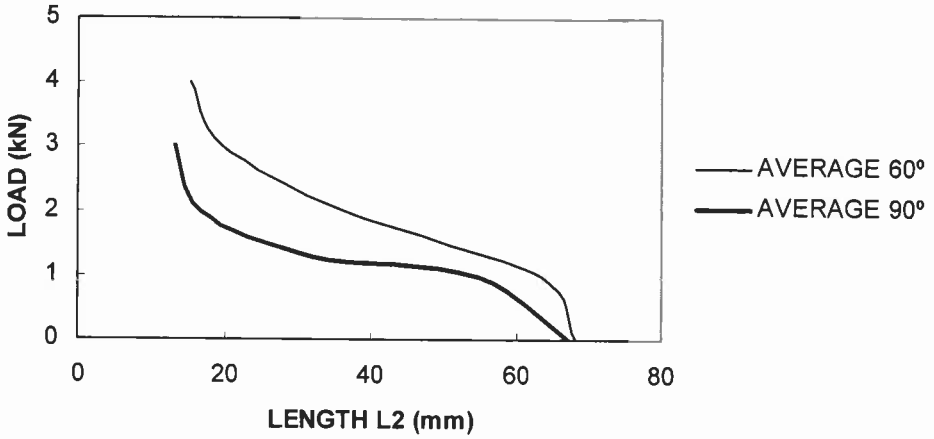

Figure 2.16 – Graphic load versus L2 length variation.

The deformation at L3 was only evaluated on specimens at 30°. The relationship between the load and the L3 length variation is represented in Figure 2.17 , where it can be seen that, for this specimen the L3 length variation was marginal because L3 is on the M1 material axis, which represents wires that were not effective in this loading versus EMS geometrical disposition.

Azurém, P – 4800-058 Guimarães
Tel. +351 253 510200 • Fax +351 253 510217

Figure 2.16 represents the relationship between the load and the length variation on L2, i.e., in the larger diagonal of the EMS module. For specimens at 60° and 90° the L2 length variation has decreased in a similar shape (see also Figures 2.10 and 2.12). Difficulties achieved on measuring the specimens at 0° and 30° prevented the evaluation of the aforementioned relationship for these specimens.

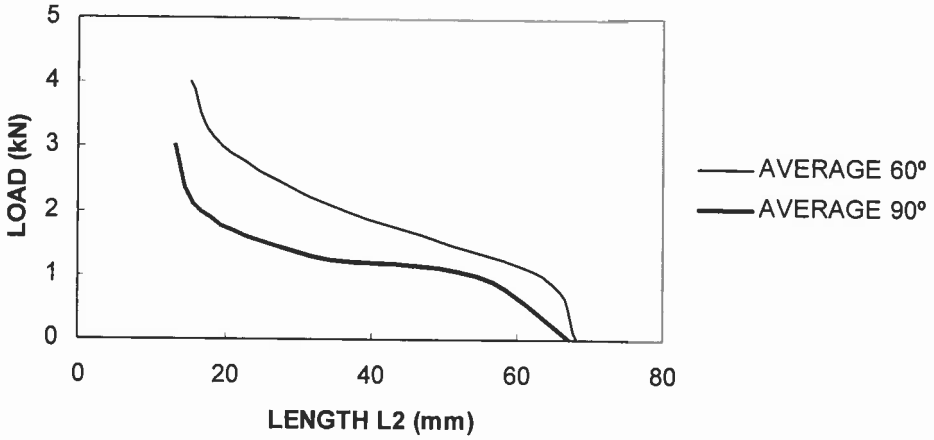

Figure 2.16 – Graphic load versus L2 length variation.

The deformation at L3 was only evaluated on specimens at 30°. The relationship between the load and the L3 length variation is represented in Figure 2.17 , where it can be seen that, for this specimen the L3 length variation was marginal because L3 is on the M1 material axis, which represents wires that were not effective in this loading versus EMS geometrical disposition.

Azurém, P – 4800-058 Guimarães
Tel. +351 253 510200 • Fax +351 253 510217

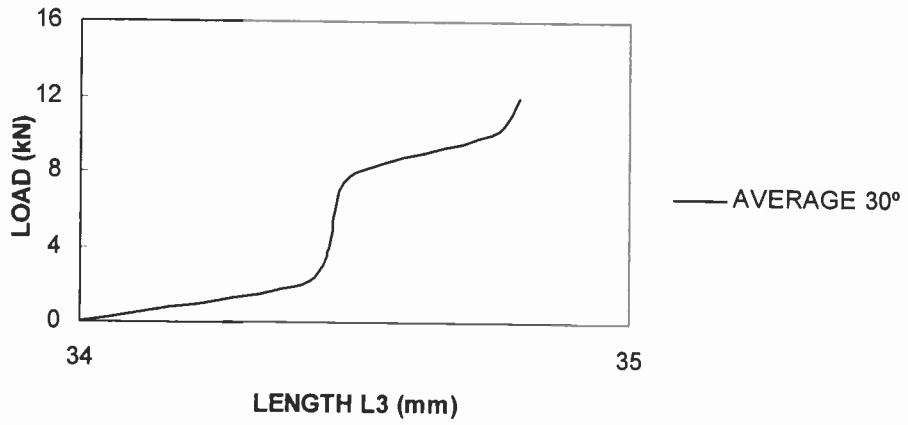

Figure 2.17 – Graphic load versus length L3 variation.

The influence of the EMS nodes was assessed measuring the L4 length variation (base length of 90mm). The relationship between the load and the L4 length variation obtained on the tests carried out is represented in Figure 2.18. The L4 length variation on the specimens at 0° decreased significantly. Part of this deformation resulted from movements at the EMS nodes. In specimens at 30° and 60° the L4 length variation was marginal because the direction of the wires where L4 was measured makes a higher angle with the loading direction (60° and 30°, respectively).

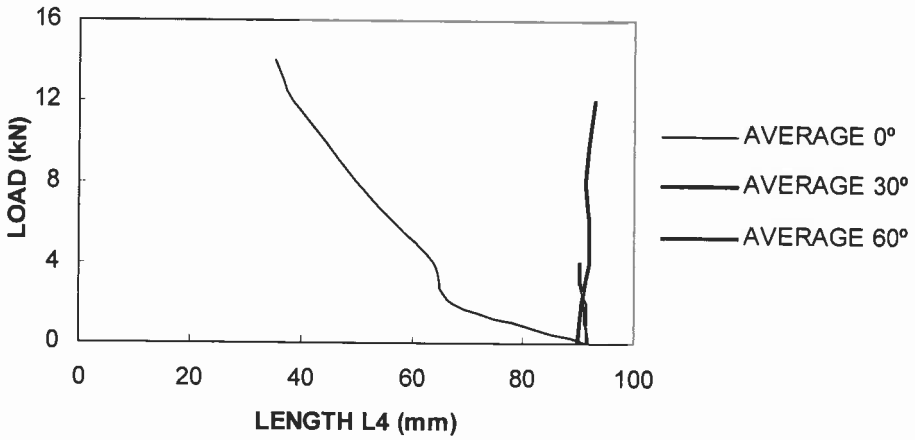

Figure 2.18 – Graphic load versus L4 length variation.

Azurém, P – 4800-058 Guimarães
Tel. +351 253 510200 • Fax +351 253 510217

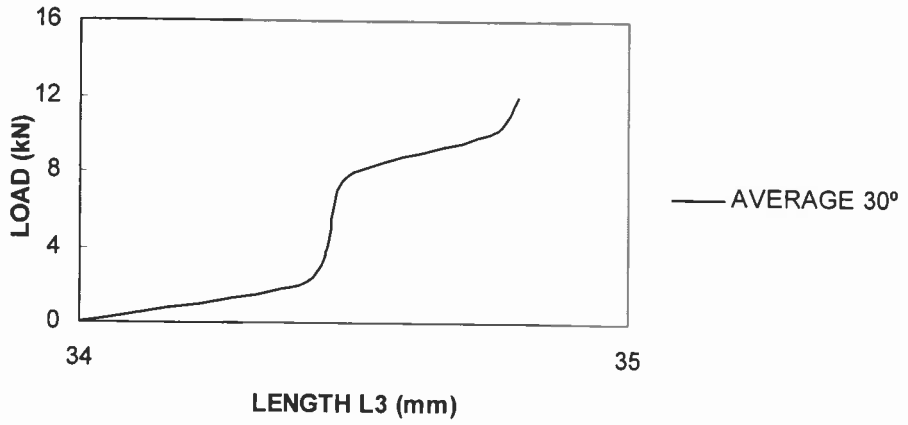

Figure 2.17 – Graphic load versus length L3 variation.

The influence of the EMS nodes was assessed measuring the L4 length variation (base length of 90mm). The relationship between the load and the L4 length variation obtained on the tests carried out is represented in Figure 2.18. The L4 length variation on the specimens at 0° decreased significantly. Part of this deformation resulted from movements at the EMS nodes. In specimens at 30° and 60° the L4 length variation was marginal because the direction of the wires where L4 was measured makes a higher angle with the loading direction (60° and 30°, respectively).

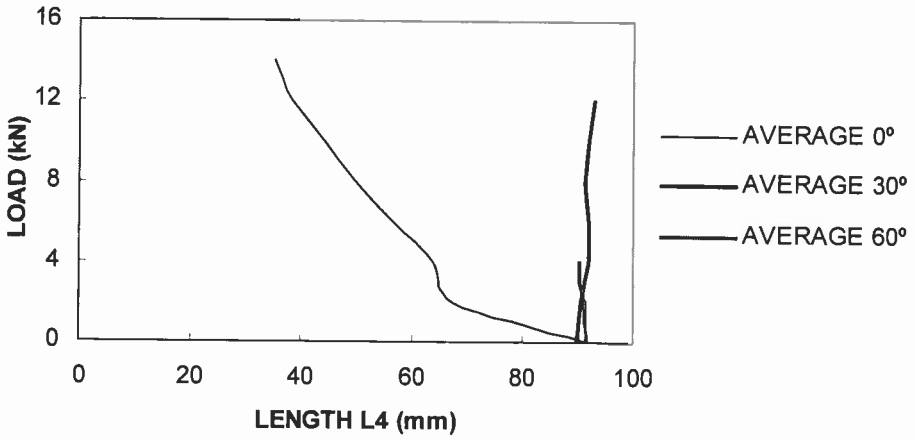

Figure 2.18 – Graphic load versus L4 length variation.

Azurém, P – 4800-058 Guimarães
Tel. +351 253 510200 • Fax +351 253 510217

3 Direct tensile tests on specimens of mortar reinforced with expanded metal sheets

To assess the effectiveness of the expanded metal sheets (EMS) for reinforcing cimentitious materials, direct tensile tests were carried out on three series of three specimens of mortar reinforced with EMS, a total of nine specimens. Amongst these series, the only significant difference was the angle between the loading direction and the geometrical axis of the EMS (0°, 30° and 60°), see Figure 1.2.

3.1 Description of the Test Set-up

To avoid excessive stress concentration in the specimens' extremities, an extra reinforcement was placed according to the arrangement illustrated in Figure 3.1. The extra reinforcement in the specimen' extremities is constituted by two layers of ϕ6mm S400 steel bars surrounding the EMS, each one having four longitudinal bars of 150mm length and three transversal bars of 200mm length, equally spaced. To avoid premature failures in front of the machine load platens, the length of the extra reinforcement is higher than the length of this fixing system, see Figure 3.2. The EMS was placed at specimen middle surface, in-between the extra reinforcement.

Azurém, P – 4800-058 Guimarães
Tel. +351 253 510200 • Fax +351 253 510217

3 Direct tensile tests on specimens of mortar reinforced with expanded metal sheets

To assess the effectiveness of the expanded metal sheets (EMS) for reinforcing cimentitious materials, direct tensile tests were carried out on three series of three specimens of mortar reinforced with EMS, a total of nine specimens. Amongst these series, the only significant difference was the angle between the loading direction and the geometrical axis of the EMS (0°, 30° and 60°), see Figure 1.2.

3.1 Description of the Test Set-up

To avoid excessive stress concentration in the specimens' extremities, an extra reinforcement was placed according to the arrangement illustrated in Figure 3.1. The extra reinforcement in the specimen' extremities is constituted by two layers of ϕ6mm S400 steel bars surrounding the EMS, each one having four longitudinal bars of 150mm length and three transversal bars of 200mm length, equally spaced. To avoid premature failures in front of the machine load platens, the length of the extra reinforcement is higher than the length of this fixing system, see Figure 3.2. The EMS was placed at specimen middle surface, in-between the extra reinforcement.

Azurém, P – 4800-058 Guimarães
Tel. +351 253 510200 • Fax +351 253 510217

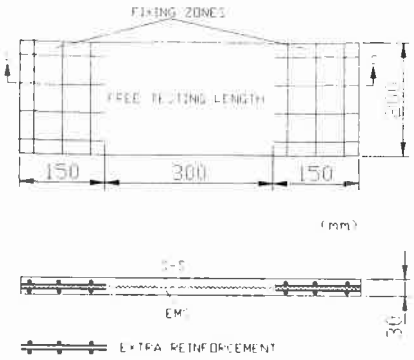

(a) (mm)

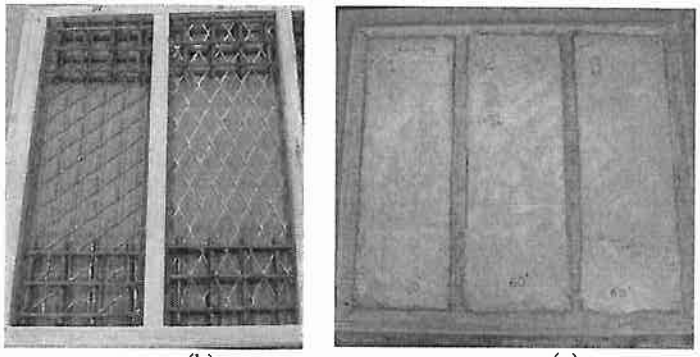

(b) (c)

Figure 3.1 – Specimens of mortar reinforced with the expanded metal sheets: (a) geometry; (b) reinforcement arrangement inside the molds; (c) specimens after cast.

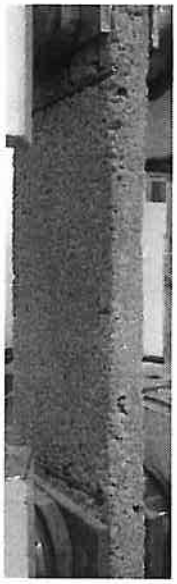

Figure 3.2 – Specimen of mortar reinforced with EMS mounted on the testing machine.

Azurém, P – 4800-058 Guimarães
Tel. +351 253 510200 • Fax +351 253 510217

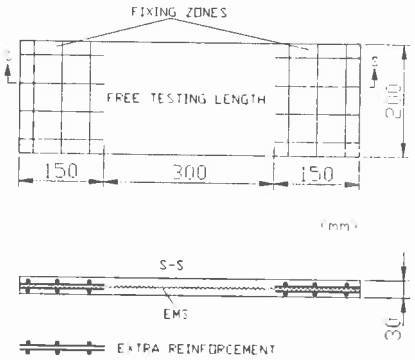

(a) (mm)

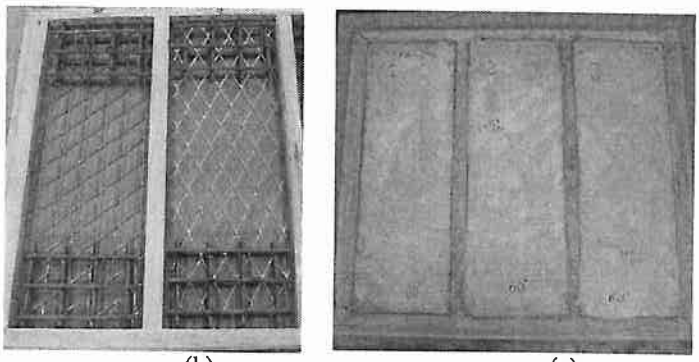

(b) (c)

Figure 3.1 – Specimens of mortar reinforced with the expanded metal sheets: (a) geometry; (b) reinforcement arrangement inside the molds; (c) specimens after cast.

Figure 3.2 – Specimen of mortar reinforced with EMS mounted on the testing machine.

Azurém, P – 4800-058 Guimarães
Tel. +351 253 510200 • Fax +351 253 510217

3.2 Mortar characterization

A mix composition of 1:3,6:12 (water:cement 42.5R:sand) was used to manufacture the mortar of the specimens, resulting a low workability mix with dry consistency. Mortar specimens of 16 × 4 × 4 cm^3 were submitted to bending tests carried out according to the European Norm (EN-196-1 (Determination of the Mechanical Strength) 1987). From the results it was obtained an average value of 2.85MPa for the flexural tensile strength. The two parts of the previous specimens, obtained after they had been tested in bending, were submitted to compression load according to EN-196-1. From the results it was verified that the mortar had an average compression strength of 35.4MPa.

3.3 Results

3.3.1 EMS at an angle of 0°

In these specimens the loading direction coincides with the G1 geometrical axis (see Figure 3.3). Several cracks, orthogonal to loading direction, have arisen along the specimen. In specimen MA2 the EMS has ruptured near their nodes that coincide with the mortar failure crack. The rupture of the EMS has occurred with low deformation of the wires crossing the mortar failure crack because its crack width was small.

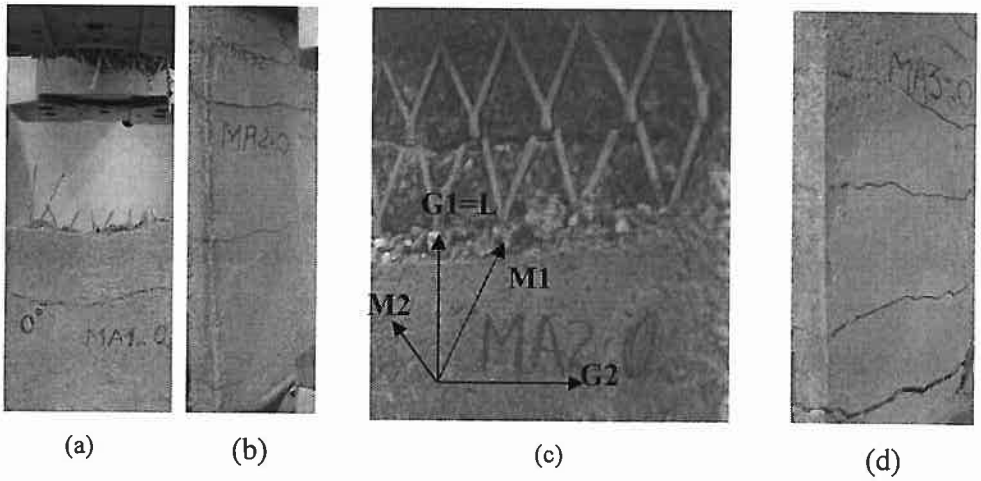

Figure 3.3 – Crack patterns and failure mode of the mortar specimens reinforced with EMS at 0°.

Azurém, P – 4800-058 Guimarães
Tel. +351 253 510200 • Fax +351 253 510217

3.2 Mortar characterization

A mix composition of 1:3,6:12 (water:cement 42.5R:sand) was used to manufacture the mortar of the specimens, resulting a low workability mix with dry consistency. Mortar specimens of 16 × 4 × 4 cm^3 were submitted to bending tests carried out according to the European Norm (EN-196-1 (Determination of the Mechanical Strength) 1987). From the results it was obtained an average value of 2.85MPa for the flexural tensile strength. The two parts of the previous specimens, obtained after they had been tested in bending, were submitted to compression load according to EN-196-1. From the results it was verified that the mortar had an average compression strength of 35.4MPa.

3.3 Results

3.3.1 EMS at an angle of 0°

In these specimens the loading direction coincides with the G1 geometrical axis (see Figure 3.3). Several cracks, orthogonal to loading direction, have arisen along the specimen. In specimen MA2 the EMS has ruptured near their nodes that coincide with the mortar failure crack. The rupture of the EMS has occurred with low deformation of the wires crossing the mortar failure crack because its crack width was small.

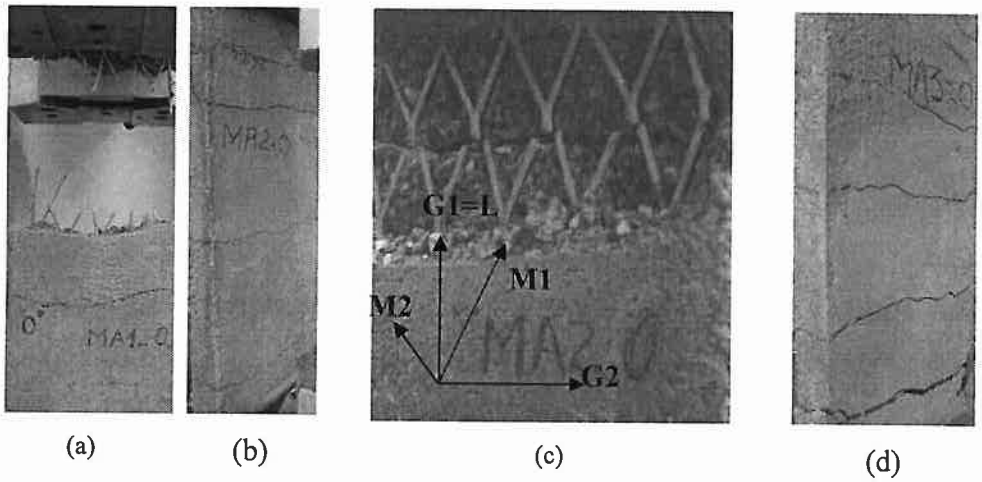

Figure 3.3 – Crack patterns and failure mode of the mortar specimens reinforced with EMS at 0°.

Azurém, P – 4800-058 Guimarães
Tel. +351 253 510200 • Fax +351 253 510217

The load-displacement relationships are depicted on Figure 3.4. After a short linear branch, the response became non-linear up to attain a "plastic" plateau at approximately 34kN, between 0.5mm and 3.0mm of displacement.

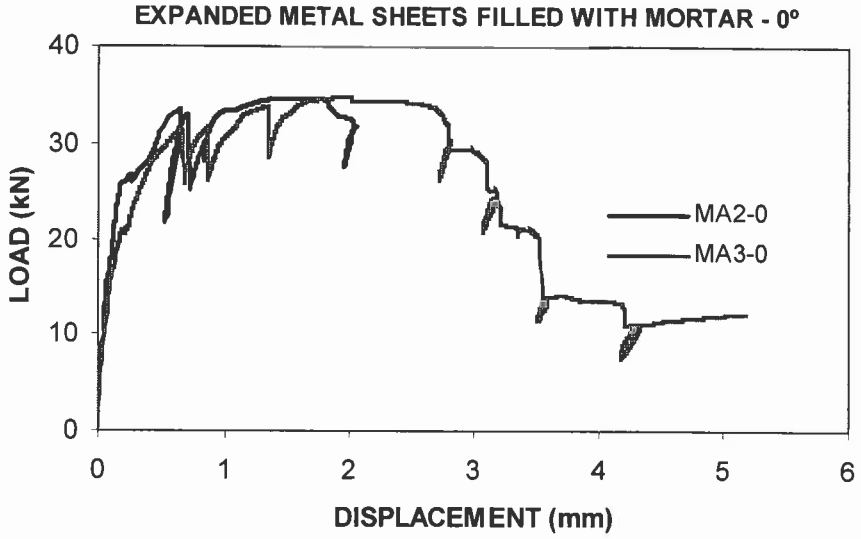

Figure 3.4 – Load versus displacement of the mortar specimens reinforced with EMS at 0°.

3.3.2 EMS at an angle of 30°

In these specimens the loading direction, L, makes 30° with the G1 EMS geometrical axis (see Figure 3.5). Figure 3.5 shows the failure modes observed on the specimens tested. It was verified a tendency for crack initiation at the specimen' extremities, followed by crack rotation into the interior of the panel (diagonal crack). This reveals that after crack initiation the principal stress directions might have changed during the loading process, due to the effects of the aggregate interlock and/or misalignment of the reinforcement crossing the cracks, motivated by the geometry variation of the EMS. The direction of the diagonal cracks is similar to the wires on the M1 direction. The crack width was even higher than the crack width on EMS specimens at 0°.

Azurém, P – 4800-058 Guimarães
Tel. +351 253 510200 • Fax +351 253 510217

The load-displacement relationships are depicted on Figure 3.4. After a short linear branch, the response became non-linear up to attain a "plastic" plateau at approximately 34kN, between 0.5mm and 3.0mm of displacement.

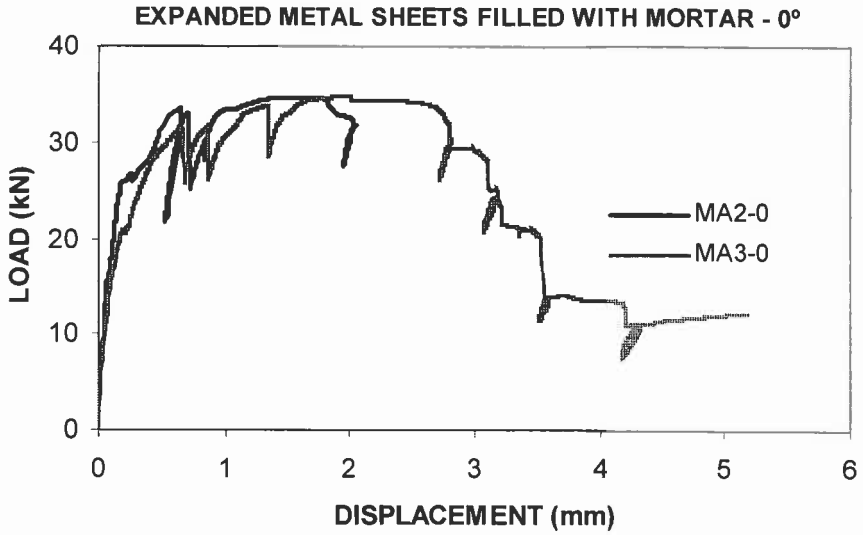

Figure 3.4 – Load versus displacement of the mortar specimens reinforced with EMS at 0°.

3.3.2 EMS at an angle of 30°

In these specimens the loading direction, L, makes 30° with the G1 EMS geometrical axis (see Figure 3.5). Figure 3.5 shows the failure modes observed on the specimens tested. It was verified a tendency for crack initiation at the specimen' extremities, followed by crack rotation into the interior of the panel (diagonal crack). This reveals that after crack initiation the principal stress directions might have changed during the loading process, due to the effects of the aggregate interlock and/or misalignment of the reinforcement crossing the cracks, motivated by the geometry variation of the EMS. The direction of the diagonal cracks is similar to the wires on the M1 direction. The crack width was even higher than the crack width on EMS specimens at 0°.

Azurém, P – 4800-058 Guimarães
Tel. +351 253 510200 • Fax +351 253 510217

Figure 3.5 – Crack patterns and failure mode of the mortar specimens reinforced with EMS at 30°.

The load-displacement relationships are depicted on Figure 3.6. It can be verified that linearity of this relationship is assured up to a load level about 8kN. Comparing the responses of the present and previous specimens it is verified that present specimens have sustained lower maximum load (about 50%). Up to a displacement of about 2.5mm the maximum load was maintained practically constant.

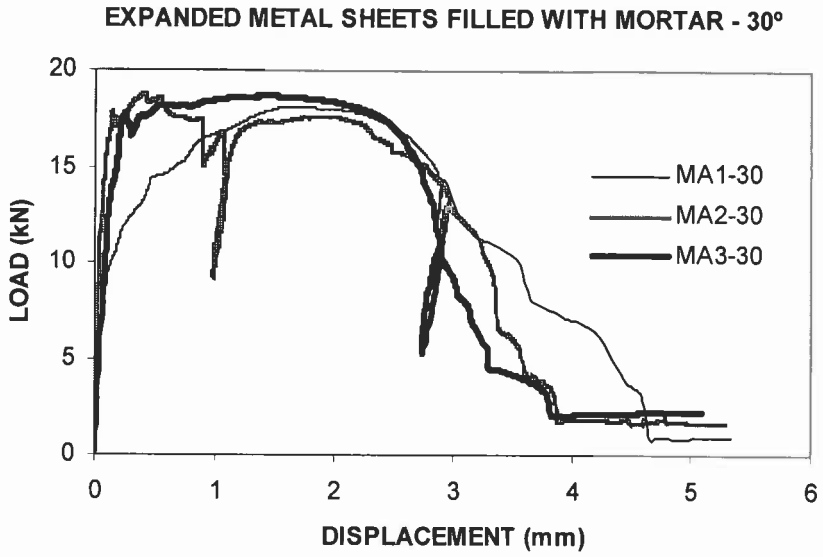

Figure 3.6 – Load versus displacement of the mortar specimens reinforced with EMS at 30°.

Azurém, P – 4800-058 Guimarães
Tel. +351 253 510200 • Fax +351 253 510217

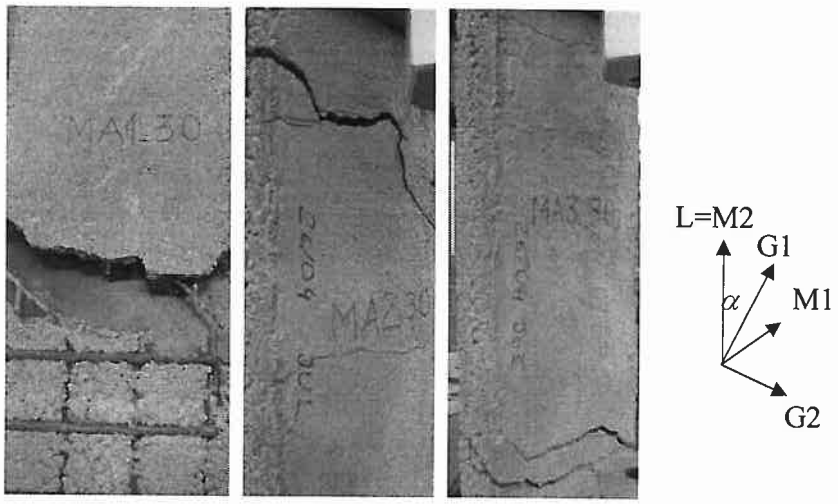

Figure 3.5 – Crack patterns and failure mode of the mortar specimens reinforced with EMS at 30°.

The load-displacement relationships are depicted on Figure 3.6. It can be verified that linearity of this relationship is assured up to a load level about 8kN. Comparing the responses of the present and previous specimens it is verified that present specimens have sustained lower maximum load (about 50%). Up to a displacement of about 2.5mm the maximum load was maintained practically constant.

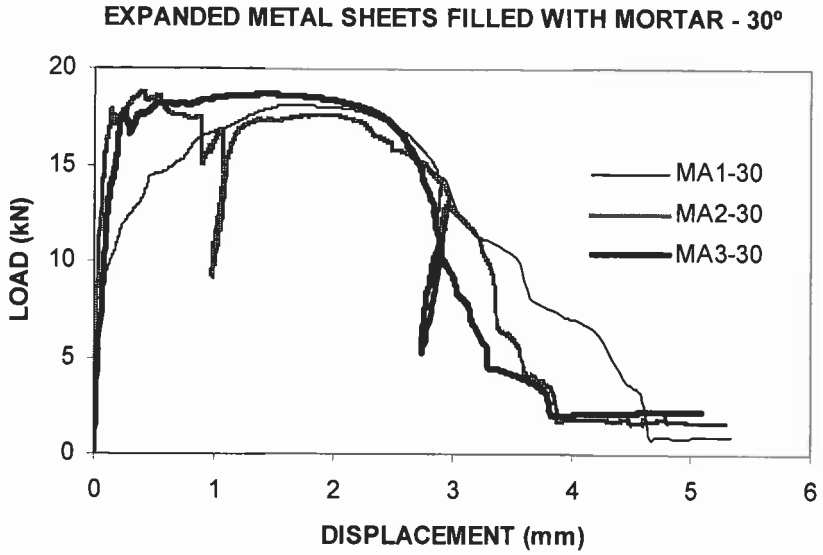

Figure 3.6 – Load versus displacement of the mortar specimens reinforced with EMS at 30°.

Azurém, P – 4800-058 Guimarães
Tel. +351 253 510200 • Fax +351 253 510217

3.3.3 EMS at an angle of 60°

In these specimens the loading direction makes 60° with the G1 EMS geometrical axis (see Figure 3.7). In these specimens the cracks concentrated at the specimen' extremities. The wires of the EMS that gave strength contribution for the specimen resistance were on M2 material direction, which makes an angle of 0° with the loading direction. When these wires were activated they have introduced shear forces that have contributed for the crack concentration on the specimen' extremities. The width of the cracks increased up to specimen rupture.

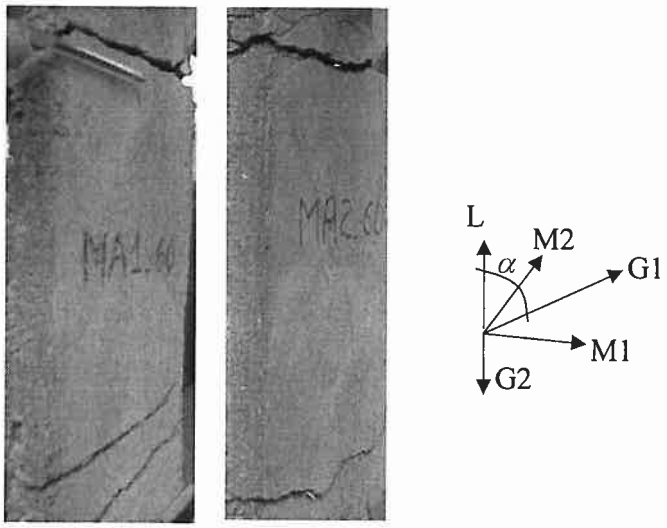

Figure 3.7 – Crack patterns and failure mode of the mortar specimens reinforced with EMS at 60°.

Azurém, P – 4800-058 Guimarães
Tel. +351 253 510200 • Fax +351 253 510217

3.3.3 EMS at an angle of 60°

In these specimens the loading direction makes 60° with the G1 EMS geometrical axis (see Figure 3.7). In these specimens the cracks concentrated at the specimen' extremities. The wires of the EMS that gave strength contribution for the specimen resistance were on M2 material direction, which makes an angle of 0° with the loading direction. When these wires were activated they have introduced shear forces that have contributed for the crack concentration on the specimen' extremities. The width of the cracks increased up to specimen rupture.

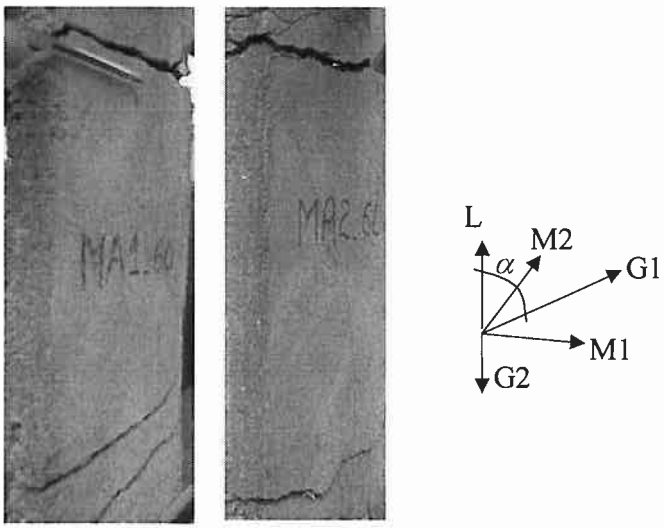

Figure 3.7 – Crack patterns and failure mode of the mortar specimens reinforced with EMS at 60°.

Azurém, P – 4800-058 Guimarães
Tel. +351 253 510200 • Fax +351 253 510217

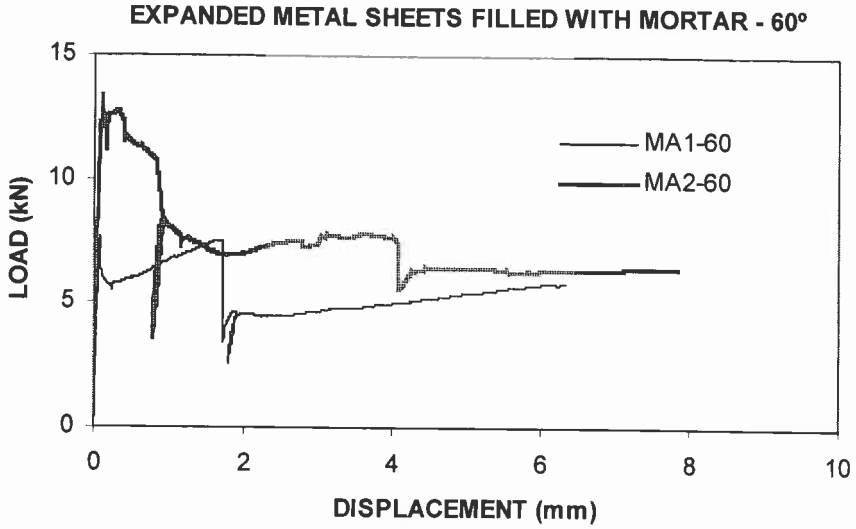

Figure 3.8 – Load versus displacement of the mortar specimens reinforced with EMS at 60°.

3.4 Analysis of the results

Figures 3.4, 3.6 and 3.8 represent the relationship between the force and the displacement measured on the machine internal transducer. Taking into account the flexural tensile strength and the compression strength of the mortar, and using the recommendations of the CEB-FIP model code it was obtained a force of 7.6kN for the crack initiation (Fcr), which is in agreement to these Figures because up to this load level the load-displacement relationships are linear.

The EMS at 0° has given a significant contribution for the load bearing capacity of the specimens. Adding the maximum force registered on the EMS specimens at 0° (see Figure 3.9) to Fcr (≈20kN) it was verified that the maximum load obtained on the mortar specimens reinforced with EMS at 0° can only be justified by the tension stiffening effect provided by the EMS.

Azurém, P – 4800-058 Guimarães
Tel. +351 253 510200 • Fax +351 253 510217

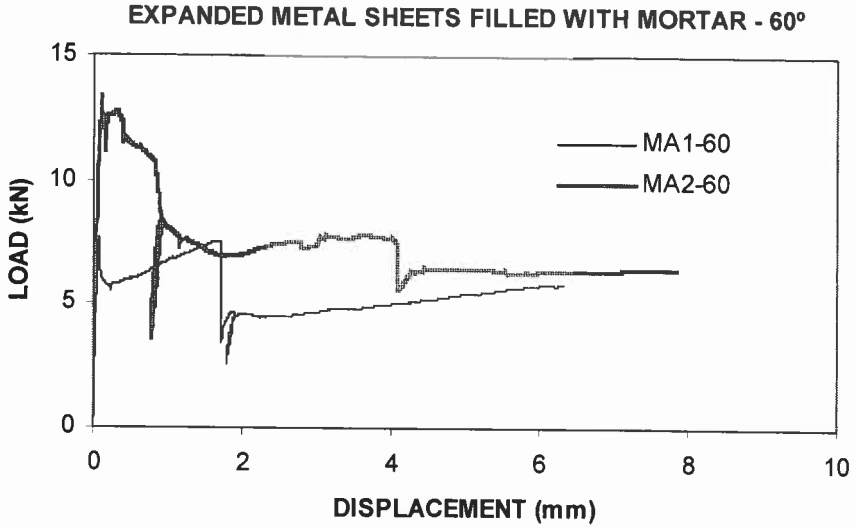

Figure 3.8 – Load versus displacement of the mortar specimens reinforced with EMS at 60°.

3.4 Analysis of the results

Figures 3.4, 3.6 and 3.8 represent the relationship between the force and the displacement measured on the machine internal transducer. Taking into account the flexural tensile strength and the compression strength of the mortar, and using the recommendations of the CEB-FIP model code it was obtained a force of 7.6kN for the crack initiation (Fcr), which is in agreement to these Figures because up to this load level the load-displacement relationships are linear.

The EMS at 0° has given a significant contribution for the load bearing capacity of the specimens. Adding the maximum force registered on the EMS specimens at 0° (see Figure 3.9) to Fcr (≈20kN) it was verified that the maximum load obtained on the mortar specimens reinforced with EMS at 0° can only be justified by the tension stiffening effect provided by the EMS.

Azurém, P – 4800-058 Guimarães
Tel. +351 253 510200 • Fax +351 253 510217

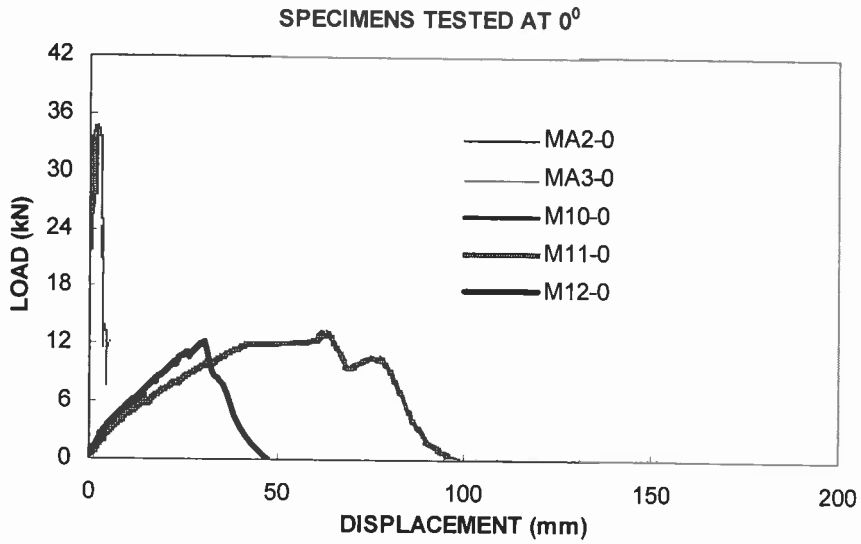

Figure 3.9 – Load-displacement relationship of the EMS specimens at 0° and mortar reinforced with EMS at 0°.

For specimens reinforced with EMS at 30° and 60° it is verified that the addition of the cracking force (Fcr) to the maximum load supported by EMS specimens at 30° 60°, respectively, (see Figure 3.10 and 3.11) gives a value near the maximum load register on the mortar specimens of these series, indicating that, for this direction of the EMS, the tension stiffening effect was negligible. In these two series the percentage of effective reinforcement crossing the failure crack is too low for giving any tension stiffening contribution (Barros, 1995).

Azurém, P – 4800-058 Guimarães
Tel. +351 253 510200 • Fax +351 253 510217

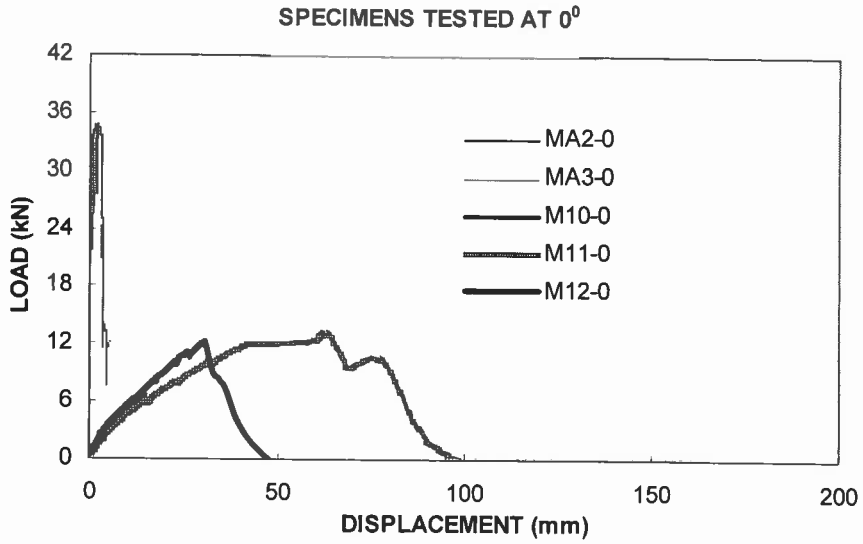

Figure 3.9 – Load-displacement relationship of the EMS specimens at 0° and mortar reinforced with EMS at 0°.

For specimens reinforced with EMS at 30° and 60° it is verified that the addition of the cracking force (Fcr) to the maximum load supported by EMS specimens at 30° 60°, respectively, (see Figure 3.10 and 3.11) gives a value near the maximum load register on the mortar specimens of these series, indicating that, for this direction of the EMS, the tension stiffening effect was negligible. In these two series the percentage of effective reinforcement crossing the failure crack is too low for giving any tension stiffening contribution (Barros, 1995).

Azurém, P – 4800-058 Guimarães
Tel. +351 253 510200 • Fax +351 253 510217

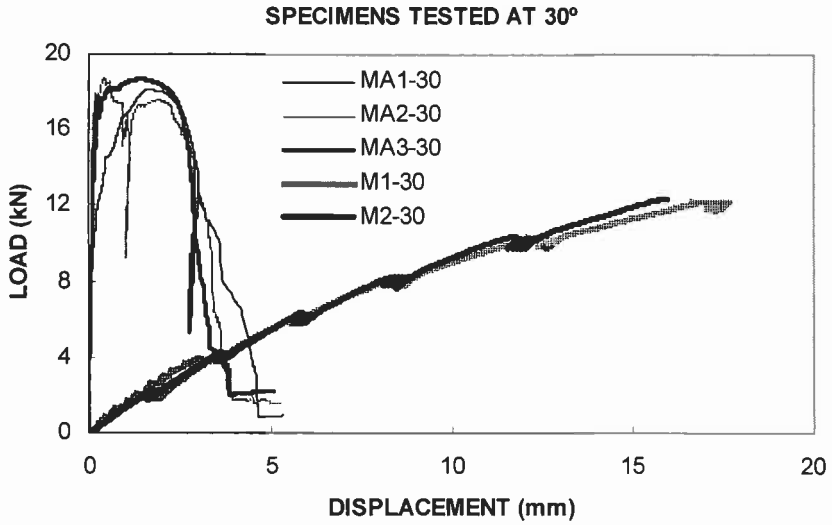

Figure 3.10 – Load-displacement relationship of the EMS specimens at 30° and mortar reinforced with EMS at 30°.

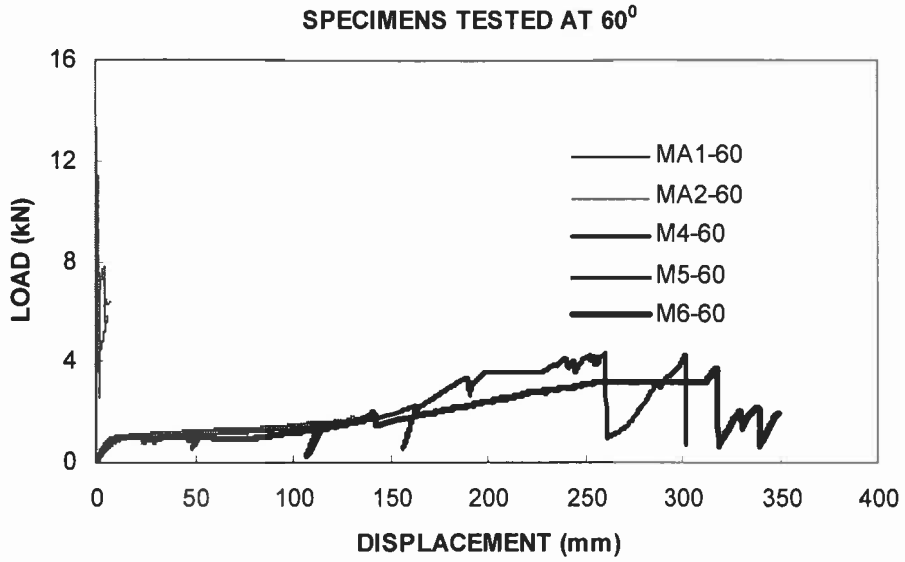

Figure 3.11 – Load-displacement relationship of the EMS specimens at 60° and mortar reinforced with EMS at 60°.

This behavior can be also explained by the decreasing cross section area of the equivalent reinforcement, $A_{s,eq}$, with the increment of the angle α ($A_{s,eq}$ = 50.63mm^2, 47.81 mm^2 and 20.25mm^2 for α= 0°, 30° and 60°). $A_{s,eq}$ is the cross section area of a

Azurém, P – 4800-058 Guimarães Tel. +351 253 510200 • Fax +351 253 510217

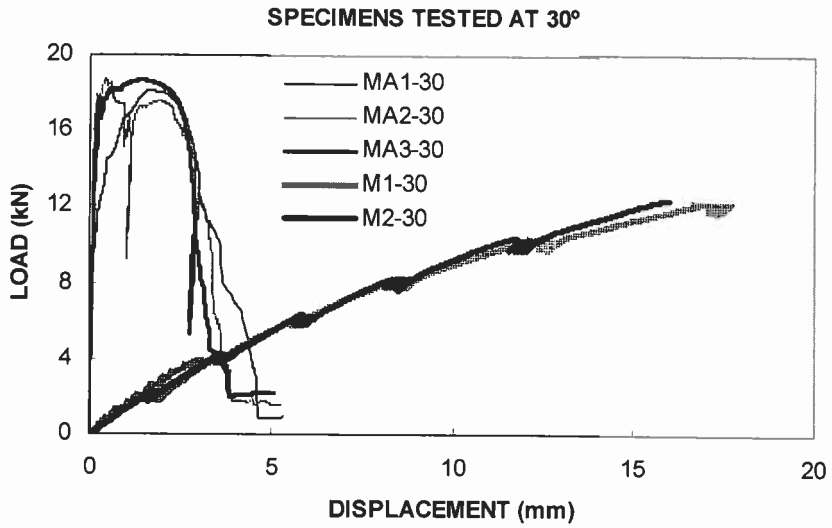

Figure 3.10 – Load-displacement relationship of the EMS specimens at 30° and mortar reinforced with EMS at 30°.

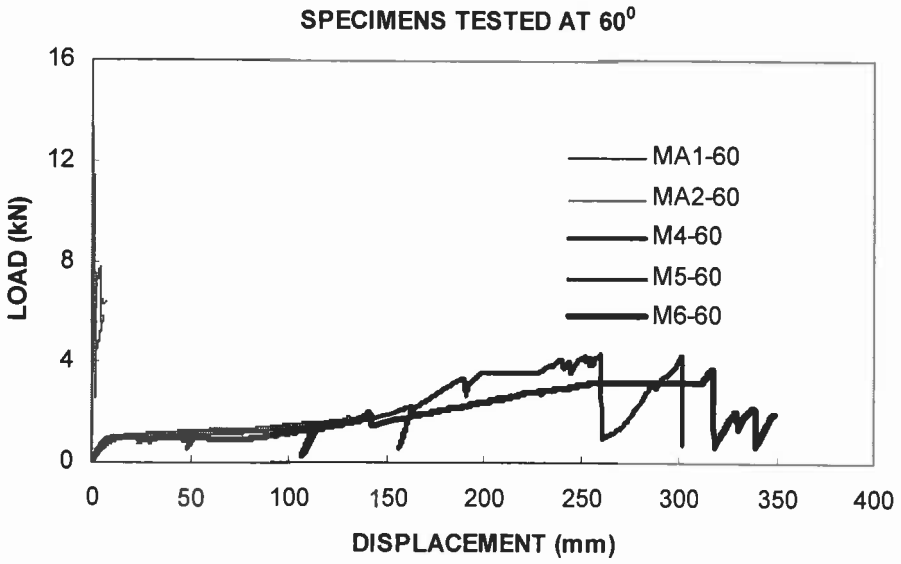

Figure 3.11 – Load-displacement relationship of the EMS specimens at 60° and mortar reinforced with EMS at 60°.

This behavior can be also explained by the decreasing cross section area of the equivalent reinforcement, $A_{s,eq}$, with the increment of the angle α ($A_{s,eq}$ = 50.63mm^2, 47.81 mm^2 and 20.25mm^2 for α= 0°, 30° and 60°). $A_{s,eq}$ is the cross section area of a

Azurém, P – 4800-058 Guimarães
Tel. +351 253 510200 • Fax +351 253 510217

fictitious reinforcement orthogonal to the crack, equivalent to the reinforcements crossing the crack, that can be evaluated from Equation 3.1 (Barros, 1995), where A_{si} is the cross section area of the reinforcement i, and θ_i is the angle between the i^{th} reinforcement and the normal to the crack surface (see Figure 3.12).

$$A_{s,eq} = \sum_{i=1}^{nr} A_{si} \cos^4 \theta_i \tag{3.1}$$

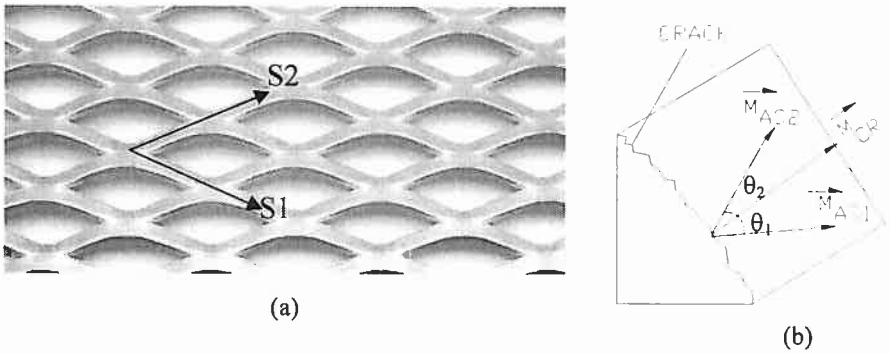

(a) (b)

Figure 3.12 – Concept of equivalent reinforcement

Unload-reload branches have occurred when cracks have arisen. In specimen MA1-30 the nonlinear response occurred for a load level lower than the one of the specimens MA2-30 and MA3-30. This might be related to the fact that a smaller number of cracks have developed on MA1-30. In comparison to the two others series, the behavior of the mortar specimens reinforced with EMS at 60° was much more brittle, because few number of cracks have occurred, due to the low value of the cross section area of the equivalent reinforcement crossing the failure crack, not enough to assured a stabilized cracking condition.

Azurém, P – 4800-058 Guimarães Tel. +351 253 510200 • Fax +351 253 510217

fictitious reinforcement orthogonal to the crack, equivalent to the reinforcements crossing the crack, that can be evaluated from Equation 3.1 (Barros, 1995), where A_{si} is the cross section area of the reinforcement i, and θ_i is the angle between the i^{th} reinforcement and the normal to the crack surface (see Figure 3.12).

$$A_{s,eq} = \sum_{i=1}^{nr} A_{si} \cos^4 \theta_i \tag{3.1}$$

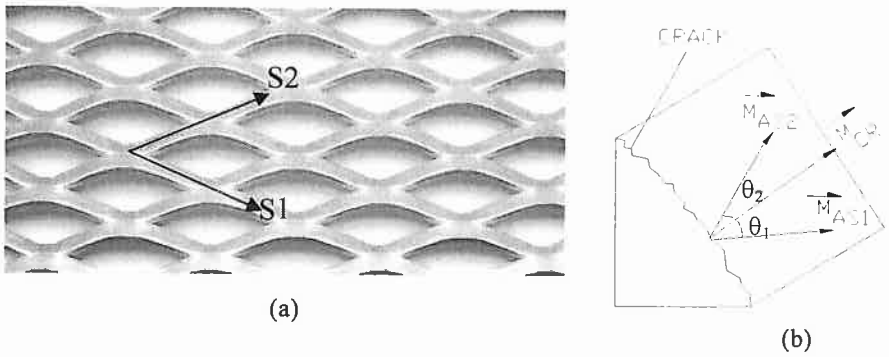

(a) (b)

Figure 3.12 – Concept of equivalent reinforcement

Unload-reload branches have occurred when cracks have arisen. In specimen MA1-30 the nonlinear response occurred for a load level lower than the one of the specimens MA2-30 and MA3-30. This might be related to the fact that a smaller number of cracks have developed on MA1-30. In comparison to the two others series, the behavior of the mortar specimens reinforced with EMS at 60° was much more brittle, because few number of cracks have occurred, due to the low value of the cross section area of the equivalent reinforcement crossing the failure crack, not enough to assured a stabilized cracking condition.

Azurém, P – 4800-058 Guimarães
Tel. +351 253 510200 • Fax +351 253 510217

Table 3.1 – Main Results obtained on the specimens of mortar reinforced with EMS.

Angle	Specimen	Maximum Load (kN)		Displacement at maximum load of the individual specimen [mm]
		Individual specimens	Average	
0°	MA1	-	34.48	-
	MA2	34.54		-
	MA3	34.42		5.17
30°	MA1	18.10	18.38	4.65
	MA2	18.49		3.94
	MA3	18.56		3.87
60°	MA1	7.46	10.39	6.33
	MA2	13.32		4.46
	MA3	-		-

4 Conclusions

Specimens of EMS

From the test carried out it was observed that the behavior of the specimens of expanded metal sheet (EMS) is deeply dependent on the load direction. The maximum value of the peak load and the minimum deformation was registered on the specimens where the load direction made an angle of 30° (α) with the G1 geometrical axis (see figure 1.2) because the M2 material axis coincides with the load direction (see figure 2.7). For EMS specimens with α=60° and 90° the load bearing capacity is too low and the deformation is too high due to an expressive geometry accommodation during the test. In specimen with α=0° the maximum load was a little bit less than the value registered on specimens with α=30°, because the wires composing the EMS have equal effectiveness in terms of reinforcement (same angle with the loading direction - see Figure 2.5). However, the deformation on specimens with α=0° was much larger than the deformation in specimens with α=30°. Using the force values at limit of proportionality and at peak load for determining an equivalent cross-section area of a fictitious conventional reinforcement

Azurém, P – 4800-058 Guimarães
Tel. +351 253 510200 • Fax +351 253 510217

Table 3.1 – Main Results obtained on the specimens of mortar reinforced with EMS.

Angle	Specimen	Maximum Load (kN)		Displacement at maximum load of the individual specimen [mm]
		Individual specimens	Average	
	MA1	-		-
0°	MA2	34.54	34.48	-
	MA3	34.42		5.17
	MA1	18.10		4.65
30°	MA2	18.49	18.38	3.94
	MA3	18.56		3.87
	MA1	7.46		6.33
60°	MA2	13.32	10.39	4.46
	MA3	-		-

4 Conclusions

Specimens of EMS

From the test carried out it was observed that the behavior of the specimens of expanded metal sheet (EMS) is deeply dependent on the load direction. The maximum value of the peak load and the minimum deformation was registered on the specimens where the load direction made an angle of 30° (α) with the G1 geometrical axis (see figure 1.2) because the M2 material axis coincides with the load direction (see figure 2.7). For EMS specimens with α=60° and 90° the load bearing capacity is too low and the deformation is too high due to an expressive geometry accommodation during the test. In specimen with α=0° the maximum load was a little bit less than the value registered on specimens with α=30°, because the wires composing the EMS have equal effectiveness in terms of reinforcement (same angle with the loading direction - see Figure 2.5). However, the deformation on specimens with α=0° was much larger than the deformation in specimens with α=30°. Using the force values at limit of proportionality and at peak load for determining an equivalent cross-section area of a fictitious conventional reinforcement

Azurém, P – 4800-058 Guimarães Tel. +351 253 510200 • Fax +351 253 510217

it was verified that for force values corresponding to acceptable deformations the reinforcement provided by EMS is too low.

Specimens of mortar reinforced with EMS

Apart the case where the EMS is at 0°, in the remaining directions of the EMS, the maximum load bearing capacity of mortar specimens reinforced with EMS is the addition of the load bearing capacity of the mortar and the EMS. Therefore, the reinforcement percentage is not enough to provide post-cracking residual strength to the mortar (tension-stiffening). As in shell applications the crack can have unpredictable orientation, the reinforcement efficacy of EMS is marginal.

5 Acknowledgements

The study presented in this report makes part of the research program "Industrialised Solutions for Construction of Masonry Shell Roofs" supported by ISO-BRICK project. The appropriate "vulcanized" rubber was generously supplied by Fernando Lemos LDA, the cement by SECIL – Companhia Geral de Cal e Cimento, S.A, Special thanks for Portuguese Science and Technology Foundation (FCT) to support the first author.

Azurém, P – 4800-058 Guimarães Tel. +351 253 510200 • Fax +351 253 510217

it was verified that for force values corresponding to acceptable deformations the reinforcement provided by EMS is too low.

Specimens of mortar reinforced with EMS

Apart the case where the EMS is at 0°, in the remaining directions of the EMS, the maximum load bearing capacity of mortar specimens reinforced with EMS is the addition of the load bearing capacity of the mortar and the EMS. Therefore, the reinforcement percentage is not enough to provide post-cracking residual strength to the mortar (tension-stiffening). As in shell applications the crack can have unpredictable orientation, the reinforcement efficacy of EMS is marginal.

5 Acknowledgements

The study presented in this report makes part of the research program "Industrialised Solutions for Construction of Masonry Shell Roofs" supported by ISO-BRICK project. The appropriate "vulcanized" rubber was generously supplied by Fernando Lemos LDA, the cement by SECIL – Companhia Geral de Cal e Cimento, S.A, Special thanks for Portuguese Science and Technology Foundation (FCT) to support the first author.

Azurém, P – 4800-058 Guimarães Tel. +351 253 510200 • Fax +351 253 510217

6 References

BARROS, J.A.O., "Comportamento de Betão Reforçado com Fibras-Análise Experimental e Simulação Numérica", PhD thesis, FEUP, December, 1995.

CEB-FIP Model Code 1990. *Comite Euro-International du Beton*, Bulletin d'Information nº 213/214, Ed. Thomas Telford, (1993).

EN 196-1, European Norm to Methods of testing cement; Determination of Strength – Part 1: Determination of mechanical strength, 1987.

RILEM. Technical Recommendations for the Testing and use of Construction Materials. International Union of Testing and Research Laboratories for Materials and Structures, 1994.

Azurém, P – 4800-058 Guimarães
Tel. +351 253 510200 • Fax +351 253 510217

6 References

BARROS, J.A.O., "Comportamento de Betão Reforçado com Fibras-Análise Experimental e Simulação Numérica", PhD thesis, FEUP, December, 1995.

CEB-FIP Model Code 1990. *Comite Euro-International du Beton*, Bulletin d'Information nº 213/214, Ed. Thomas Telford, (1993).

EN 196-1, European Norm to Methods of testing cement; Determination of Strength – Part 1: Determination of mechanical strength, 1987.

RILEM. Technical Recommendations for the Testing and use of Construction Materials. International Union of Testing and Research Laboratories for Materials and Structures, 1994.

Azurém, P – 4800-058 Guimarães
Tel. +351 253 510200 • Fax +351 253 510217